Hindawi
Mathematical Problems in Engineering
Volume 2022, Article ID 7004412, 28 pages
https://doi.org/10.1155/2022/7004412

Research Article

Approximate Analytical Solution of Two-Dimensional Nonlinear Time-Fractional Damped Wave Equation in the Caputo Fractional Derivative Operator

Alemayehu Tamirie Deresse,[1] **Yesuf Obsie Mussa**,[2] **and Ademe Kebede Gizaw**[2]

[1]*Department of Mathematics, Faculty of Natural Sciences, Mizan Tepi University, Tepi, Ethiopia*
[2]*Department of Mathematics, College of Natural Sciences, Jimma University, Jimma, Ethiopia*

Correspondence should be addressed to Alemayehu Tamirie Deresse; alemayehutamire006@gmail.com

Received 4 August 2022; Revised 5 October 2022; Accepted 6 October 2022; Published 4 November 2022

Academic Editor: José Francisco Gómez Aguilar

In this work, we proposed a new method called Laplace–Padé–Caputo fractional reduced differential transform method (LPCFRDTM) for solving a two-dimensional nonlinear time-fractional damped wave equation subject to the appropriate initial conditions arising in various physical models. LPCFRDTM is the amalgamation of the Laplace transform method (LTM), Padé approximant, and the well-known reduced differential transform method (RDTM) in the Caputo fractional derivative senses. First, the solution to the problem is gained in the convergent power series form with the help of the Caputo fractional-reduced differential transform method. Then, the Laplace–Padé approximant is applied to enlarge the domain of convergence. The advantage of this method is that it solves equations simply and directly without requiring enormous amounts of computational work, perturbations, or linearization, and it expands the convergence domain, leading to the exact answer. To confirm the effectiveness, accuracy, and convergence of the proposed method, four test-modeling problems from mathematical physics nonlinear wave equations are considered. The findings and results showed that the proposed approach may be utilized to solve comparable wave equations with nonlinear damping and source components and to forecast and enrich the internal mechanism of nonlinearity in nonlinear dynamic events.

1. Introduction

Linear and nonlinear fractional differential equations can successfully simulate fractional derivatives in a range of scientific and technical domains, including electrical networks, chemical physics, control theory of dynamical systems, reaction-diffusion, signal processing, and heat transform [1–7]. Because fractional differential equations (FDEs) often exist in several fields of engineering and science, many researchers focus their efforts on obtaining exact/approximate solutions to these dynamic fractional differential equations utilizing a variety of powerful established approaches, including the finite difference method [8], Caputo fractional-reduced differential transform method [9–11], Padé–Sumudu–Adomian decomposition method [12], triple Laplace transform method [13–15], double Sumudu transform iterative method [16], shifted Chebyshev polynomial-based method [17], Laplace decomposition method [18, 19], homotopy analysis method [20], double Laplace transform method [21], homotopy perturbation method [22, 23], conformable reduced differential transform method [24], conformable fractional-modified homotopy perturbation, Adomian decomposition method [25], differential transform method [26–28], and the new function method based on the Jacobi elliptic functions [29].

Among the approaches listed above, Keskin and Oturance were the first ones to present the Caputo FRDTM, which has been successfully utilized to solve linear and nonlinear fractional differential equations [9, 30]. Many intellectuals have implemented this method for solving various sorts of equations in recent years. For example, Kenea [31] used CFRDM to find closed solutions and accurate solutions to one-dimensional time-fractional diffusion equations with beginning conditions in the form of infinite fractional power series. CFRDTM offers the benefit of minimizing the number of computations required and offering analytic approximations, in many cases exact answers, in the form of a fast-converging power series with elegantly computed terms [32–35]. Furthermore, CFRDTM has an alternative plan to solve problems to overcome the drawbacks of well-known numerical and analytical methods such as Adomian decomposition, differential transform, homotopy perturbation, and variational iteration, which suffer from discretization, linearization, or perturbations [36–38].

The main purpose of this study is to introduce the LPCFRDTM, which is a new approach for solving the two-dimensional time-fractional nonlinear damped wave equation. The CFRDTM, the Laplace transform method, and the Padé approximant are all jointly used in this procedure. The Padé approximation has been used in a variety of domains to approximate rational series solutions; it was invented by Henri Padé [39] circa 1980. Baker [40] established the existence and convergence of subsequences. The Padé approximant method outperforms other series approximation methods and is used to manage series convergence. The authors of the paper [41] used the multivariate Padé approximation method for solving the European vanilla call option pricing problem. According to the relationships of “smaller than” or “greater than” between stock price and option exercise price, the Padé polynomials have appeared in the fractional Black-Scholes equation using the provided method. Using these polynomials, they applied the multivariate Padé approximation method and calculated numerical solutions of the fractional Black–Scholes equation for both situations. The obtained results reveal that the multivariate Padé approximation is a very quick and accurate method for the fractional Black–Scholes equation. The Padé approximants, in other words, heighten the domain of convergence of the truncated power series solution achieved via CFRDTM or other methods, leading to the exact solutions in many cases [12, 42–45].

The proposed LPCFRDTM technique has been utilized to solve the problems as follows: The CFRDTM is used to derive the solution to FDEs in convergent power series form. Second, even though the CFRDTM solution series has a high number of terms, it may converge in a narrow area. As a result, the LPCFRDTM magnifies the truncated power series’ convergence domain, typically resulting in the exact solution. We use the Laplace transform to improve the solution of convergent series generated by the CFRDTM and then form its Padé approximant to turn the transformed series into a meromorphic function. Finally, to achieve the approximate analytical solution, we use the inverse Laplace transform of the Padé approximant function. The capacity to widen the domain of convergence of solutions or include discovering exact answers is a major benefit of using this method. Also, the LPCFRDTM can obtain exact solutions without any perturbation parameters like HPM [27, 46, 47].

The generalized two-dimensional dynamical time-fractional nonlinear damped wave equation with a source term in the Caputo fractional derivative operator is taken into account in this article [48]:

$$ {}_0^C D_t^{2\alpha} u(x, y, t) + \beta {}_0^C D_t^{\alpha} u(x, y, t) = \gamma\left(D_x^2 u(x, y, t) + D_y^2 u(x, y, t)\right) + h(x, y, t, u), (x, y) \in \Omega,\ t \geq 0, \tag{1} $$

where $\Omega = \{(x, y)\colon a \leq x \leq b, c \leq y \leq d\}$.

The initial condition associated with equation (1) is given by

$$ \begin{cases} u(x, y, 0) = \varphi_0(x, y), & x, y \in \Omega, \\ {}_0^C D_t^{\alpha} u(x, y, 0) = \varphi_1(x, y), & x, y \in \Omega, \end{cases} \tag{2} $$

where $u(x, y, t)$ is the scalar variable, t is the time, and the parameters γ and β are supposed to be real numbers with $\gamma,\ \beta \geq 0. \beta$ is the alleged dissipative term. When $\beta = 0$, Equation (1) reduces to the undamped wave equation, while $\beta > 0$ to the damped one. The known functions $\varphi_0(x, y)$ and $\varphi_1(x, y)$ represent wave kinks or modes and velocity, respectively.

The remainder of this work is divided into the following sections. The fundamental definitions of fractional calculus are provided in Section 2. CFRDTM is introduced in Section 3 along with definitions and its convergence analysis in subsection 3.1. The main idea behind the Padé approximant is explained in Section 4. Section 5 explains the underlying premise of the Laplace–Padé resummation method. In Section 6, we demonstrate the proposed method’s reliability, convergence, and efficiency using four illustrative instances. Approximate analytical answers and numerical simulations are presented in tables and graphs in Sections 6.1 and 6.2, respectively. In Section 7, we have a quick discussion. Finally, a conclusion is formed in section 8.

2. Preliminaries

In this section, we will go over some essential fractional calculus definitions, which we will use in the present investigation (see [49–53]).

Definition 1. The Riemann–Liouville fractional derivative operator of $f(x)$ is given by

$$ {}_0^R D_x^{\alpha} f(x) = \frac{1}{\Gamma(m-\alpha)} \int_0^x (x-t)^{m-\alpha-1} f(t) \mathrm{d}t, \\ \cdot m - 1 < \alpha \leq m, m \in \mathbb{N}, \tag{3} $$

where the gamma function $\Gamma(z)$ is simply a generalization of the factorial real arguments and defined by

$$\Gamma(z) = \int_0^\infty e^{-t} t^{z-1} dt, \quad z > 0. \tag{4}$$

Definition 2. The Riemann–Liouville fractional integral of order $\alpha > 0$ for a function $f \in \mathbb{C}_{-1}^m$ with $m-1 < \alpha \le m, m \in \mathbb{N}$ and is defined as

$$\begin{cases} J_x^\alpha f(x) = \dfrac{1}{\Gamma(\alpha)} \displaystyle\int_0^x (x-t)^{\alpha-1} f(t) dt, & \alpha > 0, t > 0, \\ J_x^0 f(x) = f(x). \end{cases} \tag{5}$$

When trying to describe real-world issues with fractional differential equations, the Riemann–Liouville derivative has several drawbacks because it necessitates the definition of fractional order beginning conditions, which have yet to be physically explained. In their work on the theory of visco-elasticity, Caputo and Mainardi [52] suggested a modified fractional differentiation operator D_x^α to address this mismatch. With the Caputo fractional derivative, which has unambiguous physical implications, initial and boundary conditions involving integer-order derivatives can be employed.

Definition 3. From Caputo's perspective, the fractional derivative of $f(x)$ is defined as

$$ {}_0^C D_x^\alpha f(x) = \begin{cases} m \in \mathbb{N}, \\ m \in \mathbb{N}. \end{cases} \tag{6}$$

In particular, if $0 < \alpha \le 1$, then the Caputo fractional derivative of f is

$$ {}_0^C D_x^\alpha f(x) = \frac{1}{\Gamma(1-\alpha)} \int_0^x (x-t)^{-\alpha} f'(t) dt. \tag{7}$$

Lemma 1. *If* $m-1 < \alpha \le m, m \in \mathbb{N}, t > 0$ *and* $f \in \mathbb{C}_\mu^m, \quad \mu \ge -1$, *then*

$$\begin{cases} \left({}_0^C D_t^\alpha\right)\left({}_0^C D_t^\beta\right) f(t) = {}_0^C D_t^{\alpha+\beta} f(t) = \left({}_0^C D_t^\beta\right)\left({}_0^C D_t^\alpha\right) f(t), \\ {}_0^C D_t^\alpha t^\gamma = \dfrac{\Gamma(1+\gamma)}{\Gamma(1+\gamma-\alpha)} t^{\gamma-\alpha}, \ t > 0, \\ {}_0^C D_t^\alpha J_t^\alpha f(t) = f(t), \ t > 0, \\ \left(J_t^\alpha\right)\left({}_0^C D_t^\alpha\right) f(t) = f(t) - \displaystyle\sum_{k=0}^m f^{(k)}(0^+) \frac{t^k}{k!}, \quad t > 0. \end{cases} \tag{8}$$

3. Caputo Fractional-Reduced Differential Transform Method (CFRDTM)

In this section, the fundamental necessary concepts and operations of the $(2+1)-$ dimensional CFRDTM [30, 32, 43] are presented. Additionally, the convergence analysis of the CFRDTM is also presented in subsection 3.1.

Definition 4. If a function $u(x, y, t)$ is analytic and differentiated continuously with respect to the time variable $''t''$ and space variables (x, y) in the domain of interest, then let

$$U_k(x, y) = \frac{1}{\Gamma(k\alpha+1)} \left[{}_0^C D_t^{k\alpha} u(x, y, t)\right]_{t=t_0}, \tag{9}$$

where $U_k(x, y)$ is the t-dimensional spectrum function or the transformed function, ${}_0^C D_t^{k\alpha} = \partial^{k\alpha}/\partial t^{k\alpha}$ and the parameter α indicates the order of the time fractional derivative. The original function is represented by lowercase $u(x, y, t)$ in this article, whereas the transformed function is represented by uppercase $U_k(x, y)$.

Definition 5. The inverse CFRDT of a sequence $\{U_k(x, y)\}_{k=0}^\infty$ at initial time variable $t = t_0$ is provided by

$$u(x, y, t) = \sum_{k=0}^\infty U_k(x, y) (t - t_0)^{k\alpha}, \tag{10}$$

Then, combining Equations (8) and (9), we get

$$u(x, y, t) = \sum_{k=0}^\infty \frac{1}{\Gamma(k\alpha+1)} \left[{}_0^C D_t^{k\alpha} u(x, y, t)\right]_{t=t_0} (t - t_0)^{k\alpha}. \tag{11}$$

Remark 1. The function $u(x, y, t)$ is represented in real life by an infinite series of Equation (9) about $t_0 = 0$ and can be expressed as $\tilde{u}_n(x, y, t) = \sum_{k=0}^n U_k(x, y)^{k\alpha} + R_n(x, y, t)$, where the tail function $R_n(x, y, t) = \sum_{k=n+1}^\infty U_k(x, y) t^{k\alpha}$ is negligibly small.

Moreover, the inverse CFRDT of the set of $\{U_k(x, y)\}_{k=0}^n$ yields an approximation solution as follows:

$$\tilde{u}_n(x, y, t) = \sum_{k=0}^n U_k(x, y) t^{k\alpha}, \tag{12}$$

where $'n'$ is the approximate solution's order. As a result, the actual answer to the problem is obtained as follows:

$$\begin{aligned} u(x, y, t) &= \lim_{n\longrightarrow\infty} \tilde{u}_n(x, y, t) = \sum_{k=0}^\infty U_k(x, y) t^{k\alpha} \\ &= U_0(x, y) + U_1(x, y) t^\alpha + U_2(x, y) t^{2\alpha} \\ &\quad + U_3(x, y) t^{3\alpha} + \cdots. \end{aligned} \tag{13}$$

From Equation (11), the principle of the CFRDTM can be determined to be derived from the power series expansion.

Theorem 1 (see [40]). *Assume that* $F_k(x, y), G_k(x, y)$, *and* $U_k(x, y)$ *are the RDT of the functions* $f(x, y, t), g(x, y, t)$, *and* $u(x, y, t)$ *respectively, then we have the following equations:*

(i) If $f(x, y, t) = \sin u(x, y, t)$, *then*

$$F_k(x, y) = \begin{cases} \sin U_0, & \text{if} k = 0, \\ \displaystyle\sum_{k_1=0}^{k-1} \left(1 - \frac{k_1}{k}\right) G_{k_1}(x, y) U_{k-k_1}(x, y), & \text{if} k \ge 1. \end{cases} \tag{14}$$

(ii) If $g(x, y, t) = \cos u(x, y, t)$, *then*

$$G_k(x,y)=\begin{cases}\cos U_0, & \text{if}k=0,\\ -\sum_{k_1=0}^{k-1}\left(1-\frac{k_1}{k}\right)F_{k_1}(x,y)U_{k-k_1}(x,y), & \text{if}k\geq 1.\end{cases} \tag{15}$$

Remark 2. The Mittag–Leffler function, which is a generalization of the exponential function, is defined as [54]

$$\begin{aligned}E_\alpha(t)&=\sum_{k=0}^{\infty}\frac{t^k}{\Gamma(k\alpha+1)}\\&=\sum_{k=0}^{\infty}\frac{t^k}{(k\alpha)!},\quad \alpha\in\mathbb{C},\ Re(\alpha>0).\end{aligned} \tag{16}$$

For $\alpha=1, E_\alpha(t)$ reduces to e^t and $CFRDT(E_\alpha(\lambda t^\alpha))=(\lambda)^k/\Gamma(k\alpha+1)$.

Theorem 2. (*for* $\alpha=1$, *see) Caputo fractional-reduced differential transform of the initial condition.*

If $\partial^{n\alpha}/\partial t^{n\alpha}u(x,y,0)=\varphi(x,y)$, *then* $U_n(x,y)=\varphi(x,y)/\Gamma(n\alpha+1)$.

To validate the fundamental concepts of the CFRDTM, we consider the nonlinear damping wave equation (1) with the initial condition (2) by applying the features of CFRDTM listed in Table 1 and Theorem 8 on both sides of problem (1).

$$CFRDT\left({}_0^CDt_2^\alpha u(x,y,t)+\beta_0^CDt_\alpha^u(x,y,t)\right)=CFRDT\left(\gamma\left(D_x^2u(x,y,t)+D_y^2u(x,y,t)\right)+h(x,y,t,u)\right). \tag{17}$$

The CFRDT of each term in (17) is given as follows.

$$\begin{cases}CFRDT\left({}_0^CD_t^{2\alpha}u(x,y,t)\right)=CFRDT\left(\dfrac{\partial^{2\alpha}}{\partial t^{2\alpha}}u(x,y,t)\right)=\dfrac{\Gamma(\alpha k+2\alpha+1)}{\Gamma(\alpha k+1)}U_{k+2}(x,y),\\ CFRDT\left(\beta_0^CD_t^\alpha u(x,y,t)\right)=\beta CFRDT\left(\dfrac{\partial^{\alpha}}{\partial t^{\alpha}}u(x,y,t)\right)=\beta\dfrac{\Gamma[k\alpha+\alpha+1]}{\Gamma[k\alpha+1]}U_{k+1}(x,y),\\ CFRDT\left(\gamma\left(D_x^2u(x,y,t)+D_y^2u(x,y,t)\right)\right)=\gamma\left(\dfrac{\partial^2}{\partial x^2}U_k(x,y)+\dfrac{\partial^2}{\partial y^2}U_k(x,y)\right),\\ CFRDT(h(x,y,t,u))=H_k(x,y),\ k\geq 0.\end{cases} \tag{18}$$

Substituting equation (13) into equation (12), we may construct the following iteration formula:

$$\begin{aligned}&\frac{\Gamma(\alpha k+2\alpha+1)}{\Gamma(\alpha k+1)}U_{k+2}(x,y)+\beta\frac{\Gamma[k\alpha+\alpha+1]}{\Gamma[k\alpha+1]}\\ &U_{k+1}(x,y)=\gamma\left(\frac{\partial^2}{\partial x^2}U_k(x,y)+\frac{\partial^2}{\partial y^2}U_k(x,y)\right)+H_k(x,y).\end{aligned} \tag{19}$$

Solving for $U_{k+2}(x,y)$, we obtain

$$U_{k+2}(x,y)=\frac{\Gamma(\alpha k+1)}{\Gamma(\alpha k+2\alpha+1)}\left[-\beta\frac{\Gamma[k\alpha+\alpha+1]}{\Gamma[k\alpha+1]}U_{k+1}(x,y)+\gamma\left(\frac{\partial^2}{\partial x^2}U_k(x,y)+\frac{\partial^2}{\partial y^2}U_k(x,y)\right)+H_k(x,y)\right]. \tag{20}$$

Table 1: The fundamental mathematical operations of CFRDTM [32, 33, 35, 36, 43].

Original function	Transformed function
$u(x,y,t)$	$U_k(x,y) = 1/\Gamma(k\alpha+1)[{}_0^C D t^{k\alpha} u(x,y,t)]_{t=t_0}$
$w(x,y,t) = \alpha u(x,y,t) \pm \beta v(x,y,t)$	$W_k(x,y) = \alpha U_k(x,y) \pm \beta V_k(x,y)$,where $\alpha$and are constants
$w(x,y,t) = x^m y^n t^p$	$W_k(x,y) = x^m y^n \delta(k-p)$, where $\delta(k-p) = \begin{cases} 1, & \text{if } k=p, \\ 0, & \text{if } k \neq p, \end{cases}$
$w(x,y,t) = x^m y^n t^p u(x,y,t)$	$W_k(x,y) = \begin{cases} x^m y^n U_{(k-p)}(x,y), & k \geq n, \\ 0, & \text{else}, \end{cases}$
$w(x,y,t) = u(x,y,t)v(x,y,t)$	$W_k(x,y) = \sum_{r=0}^{k} U_r(x,y)V_{k-r}(x,y) = \sum_{r=0}^{k} V_r(x,y)U_{k-r}(x,y)$
$w(x,y,t) = \partial^{N\alpha}/\partial t^{N\alpha} u(x,y,t)$	$W_k(x,y) = \Gamma[k\alpha+N\alpha+1]/\Gamma[k\alpha+1]U_{k+N}(x,y)$
$w(x,y,t) = \partial^{nr}/\partial x^{nr} u(x,y,t)$	$W_k(x,y) = \partial^{nr}/\partial x^{nr} U_k(x,y)$
$w(x,y,t) = e^{\lambda t}$	$W_k(x,y) = \lambda^k/k!$, where λ is a constant
$w(x,y,t) = \sin(\alpha x + \beta y + \omega t)$	$W_k(x,y) = \omega^k/k! \sin(k\pi/2! + \alpha x + \beta y)$, where α, β, and ω are constants
$w(x,y,t) = \cos(\alpha x + \beta y + \omega t)$	$W_k(x,y) = \omega^k/k! \cos(k\pi/2! + \alpha x + \beta y)$, where α, β, and ω are constants

When we apply the CFRDT to condition (2) according to Theorem 2, we get

$$\begin{cases} U_0(x,y) = \varphi_0(x,y), \\ U_1(x,y) = \varphi_1(x,y). \end{cases} \tag{21}$$

Using Equation (15) into Equation (14) and solving the resulting system for $k = 0, 1, 2, \ldots$, we get the following $U_{k+2}(x,y)$ values:

$$\begin{aligned} U_2(x,y) &= \frac{1}{\Gamma(2\alpha+1)}\left[-\beta\Gamma[\alpha+1]\varphi_1(x,y) + \gamma\left(\frac{\partial^2}{\partial x^2}\varphi_0(x,y) + \frac{\partial^2}{\partial y^2}\varphi_0(x,y)\right) + H_0(x,y)\right], \\ U_3(x,y) &= \frac{\Gamma(\alpha+1)}{\Gamma(3\alpha+1)}\left[-\beta\frac{\Gamma[2\alpha+1]}{\Gamma[\alpha+1]}U_2(x,y) + \gamma\left(\frac{\partial^2}{\partial x^2}\varphi_1(x,y) + \frac{\partial^2}{\partial y^2}\varphi_1(x,y)\right) + H_1(x,y)\right], \end{aligned} \tag{22}$$

and so on.

Then, the inverse CFRDT of the set of values $\{U_k(x,y)\}_{k=0}^{n}$ gives the approximate solution:

$$\tilde{u}_n(x,y,t) = \sum_{k=0}^{n} U_k(x,y)t^{k\alpha}. \tag{23}$$

In the equation, $''n''$ is the order of approximation solution. Therefore, the exact solution to the considered problem can be obtained as follows:

$$\begin{aligned} u(x,y,t) = \lim_{n\longrightarrow\infty} \tilde{u}_n(x,y,t) &= \varphi_0(x,y) + \varphi_1(x,y)t^{\alpha} \\ &+ \frac{1}{\Gamma(2\alpha+1)}\left[-\beta\Gamma[\alpha+1]\varphi_1(x,y) + \gamma\left(\frac{\partial^2}{\partial x^2}\varphi_0(x,y) + \frac{\partial^2}{\partial y^2}\varphi_0(x,y)\right) + H_0(x,y)\right]t^{2\alpha} \\ &+ \frac{\Gamma(\alpha+1)}{\Gamma(3\alpha+1)}\left[-\beta\frac{\Gamma[2\alpha+1]}{\Gamma[\alpha+1]}U_2(x,y) + \gamma\left(\frac{\partial^2}{\partial x^2}\varphi_1(x,y) + \frac{\partial^2}{\partial y^2}\varphi_1(x,y)\right) + H_1(x,y)\right]t^{3\alpha} + \cdots. \end{aligned} \tag{24}$$

3.1. Convergence of the Method

Theorem 3 (see [40, 55]). *If $\varphi_k(x,y,t) = U_k(x,y)(t)^k$, then the series solution $\sum_{k=0}^{\infty}\varphi_k(x,y,t)$ stated in Equation (9) around $t_0 = 0$, $\forall k \in \mathbb{N}\cup\{0\}$.*

(i) It is convergent if $\exists\lambda, 0 < \lambda < 1$, such that $\|\varphi_{k+1}\| \leq \lambda\|\varphi_{k+1}\|$.

(ii) It is divergent if $\exists\lambda > 1$, such that $\|\varphi_{k+1}\| \geq \lambda\|\varphi_{k+1}\|$.

Definition 6 (see [40, 55]). For $k \in \mathbb{N}\cup\{0\}$, we define

$$\gamma_k = \begin{cases} \dfrac{\|\varphi_{k+1}\|}{\|\varphi_k\|} = \dfrac{\left\|U_{k+1}(x,y)t^{k+1}\right\|}{\left\|U_k(x,y)t^k\right\|}, & \text{if}\|\varphi_k\| \neq 0, \\ 0, & \text{if}\|\varphi_k\| = 0, \end{cases} \tag{25}$$

and then, the series solution $\sum_{k=0}^{\infty}\varphi_k(x,y,t)$ converges to the exact solution $u(x,y,t)$ when $0\le\gamma_k<1$ for $k=0,1,2,\ldots$.

4. Pade Approximate

In numerical mathematics, Padé approximation [56] is believed to be the best approximation of a function by rational functions of a given order. Under this technique, the approximate power series agrees with the power series of the function it is approximating. The Padé approximant often gives a better approximation of the function than truncating its Taylor series, and it may still work where the Taylor series does not converge and also enlarges the domain of convergence of the truncated power series solution. For such reasons, Padé approximants are often used in many fields of computations.

Let $u(x,y,t)$ be an analytical function with Maclaurin's expansion.

$$u(x,y,t)=\sum_{k=0}^{\infty}u_k(x,y,t)t^k,\quad 0\le t\le T, \tag{26}$$

Then, the Padé approximant to $u(x,y,t)$ of order $[K/L]$, which is denoted as $[K/L]_u(x,y,t)$, is defined as follows [40, 42]:

$$\left[\frac{K}{L}\right]_u(x,y,t)=\frac{p_0+p_1t+p_2t^2+\cdots+p_Kt^K}{q_0+q_1t+q_2t^2+\cdots+q_Lt^L}, \tag{27}$$

where we considered $q_0=1$, and the numerator and denominator have no common factors. The numerator and the denominator in equation (19) are built in such a way that $u(x,y,t)$, $[K/L]_u(x,y,t)$, and their derivatives agree at $t=0$ up to $K+L$. That is,

$$\sum_{k=0}^{\infty}u_k(x,y,t)t^k=\frac{p_0+p_1t+p_2t^2+\cdots+p_Kt^K}{1+q_1t+q_2t^2+\cdots+q_Lt^L}+O\left(t^{K+L+1}\right). \tag{28}$$

By cross multiplying, we find that

$$\left(u_0+u_1t+u_2t^2+\cdots.\right)\left(1+q_1t+q_2t^2+\cdots+q_Lt^L\right)=p_0+p_1t+p_2t^2+\cdots+p_Kt^K+O\left(t^{K+L+1}\right). \tag{29}$$

Equating the coefficients of $t^{K+1},t^{K+2},\ldots,t^{K+L}$ from (29), we find

$$\begin{cases} u_Kq_1+u_{K+1}q_2+u_{K+2}q_3+\cdots+u_{K-L+1}q_L=-u_{K+1},\\ u_{K+1}q_1+u_{K+2}q_2+u_{K+3}q_3+\cdots+u_{K-L+2}q_L=-u_{K+2},\\ u_{K+2}q_1+u_{K+3}q_2+u_{K+4}q_3+\cdots+u_{K-L+3}q_L=-u_{K+3},\\ .\\ .\\ .\\ u_{K+L-1}q_1+u_{K+L-2}q_2+u_{K+L-3}q_3+\cdots+u_Kq_L=-u_{K+L}. \end{cases} \tag{30}$$

Comparing the equal power of "t" on both sides of (29), we get

$$\begin{cases} p_0=u_0,\\ p_1=u_1+u_0q_1,\\ p_2=u_2+u_1q_1+u_0q_2,\\ p_3=u_3+u_2q_1+u_1q_2+u_0q_3,\\ .\\ .\\ .\\ p_K=u_K+u_{K-1}q_1+u_{K-2}q_2+u_{K-3}q_3+\cdots+u_0q_K. \end{cases} \tag{31}$$

Moreover, from Equation (22), first, we calculate all the coefficients $q_n, 1\le n\le L$, and then, we determine the coefficients $p_n, 0\le n\le K$ from Equation (23).

Remark 3. For a fixed value of $K+L+1$, error equation (20) is the smallest when the numerator and denominator of Equation (14) have the same degree or when the numerator has one degree higher than the denominator.

5. Laplace–Pade Resummation Method

The LPCFRDTM, which is a combination of the CFRDTM and the Laplace–Padé resummation method, is described as follows:

(i) By means of CFRDTM, we first find the series solution of the given equation that is similar to series (16)

(ii) Second, power series (16) is transformed using the Laplace transformation

(iii) Next, we replace s by $1/t$ in the resulting equation

(iv) The series produced from (3) is then transformed into a meromorphic function by constructing its Padé approximant of order $[K/L]$, where K and L are chosen at random but should be smaller than the series' order

(v) After that, in the resulting equation, we substitute t by $1/s$

(vi) As a final point, we obtain the precise or approximate answer by applying the inverse Laplace s transformation

6. Illustrative Examples

We offer four examples to establish the validity and efficiency of the suggested strategy. These cases' solutions are also compared with exact solutions.

6.1. Analytical Solution to Illustrative Examples

Example 1. Consider the following $(2+1)$–dimensional hyperbolic time-fractional telegraph equation in the region $\Omega = [0,2]^2$ as follows:

$$\begin{aligned}{}_0^C D_t^{2\alpha} u(x,y,t) + 2\,{}_0^C D_t^{\alpha} u(x,y,t) &= D_x^2 u(x,y,t) \\ &\quad + D_y^2 u(x,y,t) - u^2 + e^{2(x+y)} \left(E_\alpha\left(-2t^\alpha\right)\right)^2 \\ &\quad - 2e^{(x+y)} \left(E_\alpha\left(-2t^\alpha\right)\right),\end{aligned} \tag{32}$$

Under the initial condition, we get

$$\begin{cases} u(x,y,0) = e^{x+y}, \\ {}_0^C D_t^{\alpha} u(x,y,0) = \dfrac{-2}{\Gamma(\alpha+1)} e^{x+y}. \end{cases} \tag{33}$$

Applying the properties of CFRDT listed in Table 1 on both sides of Equation (24), we obtain

$$U_{k+2}(x,y) = \frac{\Gamma(\alpha k+1)}{\Gamma(\alpha k+2\alpha+1)} \left[\begin{array}{c} -2\dfrac{\Gamma[k\alpha+\alpha+1]}{\Gamma[k\alpha+1]} U_{k+1}(x,y) + \dfrac{\partial^2}{\partial x^2} U_k(x,y) + \dfrac{\partial^2}{\partial y^2} U_k(x,y) \\ -\displaystyle\sum_{r=0}^{k} U_r(x,y) U_{k-r}(x,y) + e^{2(x+y)} \sum_{r=0}^{k} V_r(x,y) V_{k-r}(x,y) - 2e^{(x+y)} \left(\dfrac{(-2)^k}{\Gamma(k\alpha+1)}\right) \end{array}\right], \tag{34}$$

where $V_k(x,y)$ is the Caputo fractional-reduced transform of $E_\alpha(-2t^\alpha)$, and it is obtained by using Remark 2.

When the CFRDT is applied to initial condition (25) in view of Theorem 2, it produces

$$\begin{cases} U_0(x,y) = e^{x+y}, \\ U_1(x,y) = \dfrac{-2}{\Gamma(\alpha+1)} e^{x+y}. \end{cases} \tag{35}$$

We get the following $U_k(x,y)$ values for $k = 0,1,2,\ldots$ using Equation (27) into Equation (26), recursively.

For $k = 0$, using the values of $U_0(x,y)$ and $U_1(x,y)$ from (35) into Equation (26), we get

$$\begin{aligned} U_2(x,y) &= \frac{\Gamma(1)}{\Gamma(2\alpha+1)} \left[\begin{array}{c} -2\dfrac{\Gamma[\alpha+1]}{\Gamma(1)} U_1(x,y) + \dfrac{\partial^2}{\partial x^2} U_0(x,y) + \dfrac{\partial^2}{\partial y^2} U_0(x,y) \\ -U_0(x,y) U_0(x,y) + e^{2(x+y)} V_0(x,y) V_0(x,y) - 2e^{(x+y)} \left(\dfrac{(-2)^0}{\Gamma(1)}\right) \end{array}\right] \\ &= \frac{1}{\Gamma(2\alpha+1)} \left[\begin{array}{c} -2\Gamma(\alpha+1) \dfrac{-2}{\Gamma(\alpha+1)} e^{x+y} + \dfrac{\partial^2}{\partial x^2}\left(e^{x+y}\right) + \dfrac{\partial^2}{\partial y^2}\left(e^{x+y}\right) \\ -\left(e^{x+y}\right)\left(e^{x+y}\right) + e^{2(x+y)} \dfrac{(-2)^0}{\Gamma(1)} \dfrac{(-2)^0}{\Gamma(1)} - 2e^{(x+y)} \left(\dfrac{(-2)^0}{\Gamma(1)}\right) \end{array}\right] \\ &= \frac{1}{\Gamma(2\alpha+1)} \left[4e^{x+y} + 2e^{x+y} - e^{2(x+y)} + e^{2(x+y)} - 2e^{(x+y)}\right] = \frac{2}{\Gamma(2\alpha+1)} e^{x+y}, \end{aligned} \tag{36}$$

for $k=1$, using the values of $U_1(x,y)$ and $U_2(x,y)$ in Equation (26), we obtain

$$\begin{aligned}
U_3(x,y) &= \frac{\Gamma(\alpha+1)}{\Gamma(3\alpha+1)}\left[\begin{array}{c} -2\dfrac{\Gamma[2\alpha+1]}{\Gamma[\alpha+1]}U_2(x,y)+\dfrac{\partial^2}{\partial x^2}U_1(x,y)+\dfrac{\partial^2}{\partial y^2}U_1(x,y) \\ -\displaystyle\sum_{r=0}^{1}U_r(x,y)U_{1-r}(x,y)+e^{2(x+y)}\sum_{r=0}^{1}V_r(x,y)V_{1-r}(x,y)-2e^{(x+y)}\left(\dfrac{(-2)^1}{\Gamma(\alpha+1)}\right)\end{array}\right] \\
&= \frac{\Gamma(\alpha+1)}{\Gamma(\alpha+2\alpha+1)}\left[\begin{array}{c} -2\dfrac{\Gamma[2\alpha+1]}{\Gamma[\alpha+1]}\dfrac{(-2)^2}{\Gamma(2\alpha+1)}e^{x+y}+\dfrac{-2}{\Gamma(\alpha+1)}\dfrac{\partial^2}{\partial x^2}\left(e^{x+y}\right)+\dfrac{-2}{\Gamma(\alpha+1)}\dfrac{\partial^2}{\partial y^2}\left(e^{x+y}\right) \\ -2U_0(x,y)U_1(x,y)+2e^{2(x+y)}V_0(x,y)V_1(x,y)-2e^{(x+y)}\left(\dfrac{(-2)^1}{\Gamma(\alpha+1)}\right)\end{array}\right] \\
&= \frac{\Gamma(\alpha+1)}{\Gamma(\alpha+2\alpha+1)}\left[\frac{(-2)^3}{\Gamma[\alpha+1]}e^{x+y}-4\frac{e^{x+y}}{\Gamma(\alpha+1)}+4\frac{e^{x+y}}{\Gamma(\alpha+1)}-4\frac{e^{2(x+y)}}{\Gamma(\alpha+1)}+4\frac{e^{(x+y)}}{\Gamma(\alpha+1)}\right] \\
&= \frac{(-2)^3e^{x+y}}{\Gamma(\alpha+2\alpha+1)}.
\end{aligned} \tag{37}$$

Continuing in the same manner for $k\geq 2$, we obtain

$$\begin{aligned}
U_4(x,y) &= \frac{(-2)^4}{\Gamma(4\alpha+1)}e^{x+y}, \\
U_5(x,y) &= \frac{(-2)^5}{\Gamma(5\alpha+1)}e^{x+y},\ldots,U_k(x,y)=\frac{(-2)^k}{\Gamma(k\alpha+1)}e^{x+y}.
\end{aligned} \tag{38}$$

Then, using the inverse CFRDT (9) as a definition, we get.

$$\begin{aligned}
u(x,y,t) &= \sum_{k=0}^{\infty}U_k(x,y)(t)^{k\alpha} \\
&= e^{x+y}\left[1+\frac{(-2)t^\alpha}{\Gamma(\alpha+1)}+\frac{(-2)^2t^{2\alpha}}{\Gamma(2\alpha+1)}+\frac{(-2)^3t^{3\alpha}}{\Gamma(3\alpha+1)}+\frac{(-2)^4t^{4\alpha}}{\Gamma(4\alpha+1)}+\frac{(-2)^5t^{5\alpha}}{\Gamma(5\alpha+1)}+\cdots\right] \\
&= e^{x+y}\left(\sum_{k=0}^{\infty}\frac{(-2)^k(t)^{k\alpha}}{\Gamma(k\alpha+1)}\right).
\end{aligned} \tag{39}$$

In this situation, the truncated series is approximated using the Laplace–Padé approximant up to n^{th} order of perturbation. That is,

$$\tilde{u}_n(x,y,t)=e^{x+y}\left(\sum_{k=0}^{n}\frac{(-2)^k(t)^{k\alpha}}{\Gamma(k\alpha+1)}\right). \tag{40}$$

After that, we apply the Laplace transform to both sides of (40), and we get

$$L(\tilde{u}_n(x,y,t))=e^{x+y}\left(\sum_{k=0}^{n}\frac{(-2)^k}{s^{\alpha k+1}}\right). \tag{41}$$

For straightforwardness, we write $1/t$ in the place of $\mathbf{s}$ in Equation (31), and we get

$$L(\tilde{u}_n(x,y,t)) = e^{x+y}\left(\sum_{k=0}^{n}(-2)^k t^{k\alpha+1}\right), = e^{x+y}\big(t - 2t^{\alpha+1} + 2^2t^{2\alpha+1} - 2^3t^{3\alpha+1} + 2^4t^{4\alpha+1} - 2^5t^{5\alpha+1} + \ldots\big). \tag{42}$$

Now, we convert transformed series (32) into a meromorphic function by forming its Padé approximant of $[K/L]$ with $k \geq 1, L \geq 1$ and $K + L = 7 (k = 3, L = 4)$.

$$\left[\frac{K}{L}\right]\big(t - 2t^{\alpha+1} + 2^2t^{2\alpha+1} - 2^3t^{3\alpha+1} + 2^4t^{4\alpha+1} - 2^5t^{5\alpha+1} + 2^6t^{6\alpha+1}\big) = \frac{p_0 + p_1t + p_2t^{\alpha+1} + p_3t^{2\alpha+1}}{1 + q_1t + q_2t^{\alpha+1} + q_3t^{2\alpha+1} + q_4t^{3\alpha+1}}. \tag{43}$$

We obtain $u_0 = 0, u_1 = 1, u_2 = -2, u_3 = 4, u_4 = -8, u_5 = 16, u_6 = -32, u_7 = 64$.

Using (23) and (22), we get

$$\left\{\begin{array}{ll} p_0 = u_0 = 0, & 4q_1 - 2q_2 + q_3 + 0 = 8, \\ p_1 = 1, & -8q_1 + 4q_2 - 2q_3 + q_4 = -16, \\ p_2 = -2 + q_1, \quad \text{and} & 16q_1 - 8q_2 + 4q_3 - 2q_4 = 32, \\ p_3 = 4 - 2q_1 + q_2, & -32q_1 + 16q_2 - 8q_3 + 4q_4 = -64. \end{array}\right\}. \tag{44}$$

Solving for p and q, we obtain $p_0 = 0$, $p_1 = 1, p_2 = 0, p_3 = 1, q_1 = 2, q_2 = 1, q_3 = 2$, and $q_4 = 0$.

Then, we obtain

$$\left[\frac{K}{L}\right]\big(t - 2t^{\alpha+1} + 2^2t^{2\alpha+1} - 2^3t^{3\alpha+1} + 2^4t^{4\alpha+1} - 2^5t^{5\alpha+1} + 2^6t^{6\alpha+1}\big) = \frac{t + t^{2\alpha+1}}{1 + 2t + t^{\alpha+1} + 2t^{2\alpha+1}} = \frac{t}{1 + 2(t)^{\alpha}}. \tag{45}$$

Therefore, all $[K/L]$Padé approximants of the eqaution with $L \geq 1,\ K \geq 1$ and $K + L \leq n$ give

$$\left[\frac{K}{L}\right]_{\tilde{u}_n}(x,y,t) = \frac{e^{x+y}t}{1 + 2(t)^{\alpha}}. \tag{46}$$

Now, by changing $1/s$ into $\mathbf{t}$ in the equation, we obtain $[K/L]_{\tilde{u}_n}$ in terms of $\mathbf{s}$ as follows:

$$\left[\frac{K}{L}\right]_{\tilde{u}_n}(x,y,t) = \frac{e^{x+y}s^{\alpha-1}}{s^{\alpha} + 2}. \tag{47}$$

Finally, on both sides of Equation (34), using the inverse Laplace transform, we have the exact solution as follows:

$$u(x,y,t) = e^{x+y}L^{-1}\left\{\frac{s^{\alpha-1}}{s^{\alpha} + 2}\right\} = e^{x+y}E_{\alpha}(-2t^{\alpha}). \tag{48}$$

Putting $\alpha = 1$ in Equation (35), we obtain

$$u(x,y,t) = e^{x+y}L^{-1}\left\{\frac{1}{s + 2}\right\} = e^{x+y-2t}. \tag{49}$$

Example 2. Consider the following two-dimensional hyperbolic nonlinear time-fractional sine-Gordon equation on the domain $\Omega = [0,2]^2, \quad t \geq 0$

$$\begin{aligned} {}_0^C D_t^{2\alpha}u(x,y,t) + {}_0^C D_t^{\alpha}u(x,y,t) = {} & D_x^2 u(x,y,t) + D_y^2 u(x,y,t) - 2\sin u \\ & + 2\sin\left[E_{\alpha}(-t^{\alpha})(1 - \cos(\pi x))(1 - \cos(\pi y))\right] \\ & - \pi^2 E_{\alpha}(-t^{\alpha})\left[\cos(\pi x) + \cos(\pi y) - 2\cos(\pi x)\cos(\pi y)\right]. \end{aligned} \tag{50}$$

Under the initial condition, we get

$$\begin{cases} u(x,y,0) = (1-\cos(\pi x))(1-\cos(\pi y)), \\ {}_0^C D_t^{\alpha} u(x,y,0) = -\dfrac{1}{\Gamma(\alpha+1)}(1-\cos(\pi x))(1-\cos(\pi y)). \end{cases} \quad (51)$$

Applying the properties of CFRDT listed in Table 1, Theorem 1, and Definition 4 on both sides of Equation (37), we obtain

$$U_{k+2}(x,y) = \frac{\Gamma(\alpha k+1)}{\Gamma(\alpha k+2\alpha+1)}\left[-\frac{\Gamma[k\alpha+\alpha+1]}{\Gamma[k\alpha+1]}U_{k+1}(x,y) + \frac{\partial^2}{\partial x^2}U_k(x,y) + \frac{\partial^2}{\partial y^2}U_k(x,y) - 2F_k(x,y) + H_k(x,y)\right], \quad (52)$$

where $F_k(x,y)$ and $H_k(x,y)$ are transformed forms of nonlinear term $\sin(u(x,y,t))$ and $[[2\sin(E_\alpha(-t^\alpha)((1-\cos(\pi x))(1-\cos(\pi y))))] - \pi^2 E_\alpha(-t^\alpha)[\cos(\pi x) + \cos(\pi y) - 2\cos(\pi x)\cos(\pi y)]]$, respectively. Applying the CFRDT to initial condition (38) in view of Theorem 2, we get

$$\begin{cases} U_0(x,y) = (1-\cos(\pi x))(1-\cos(\pi y)), \\ U_1(x,y) = -\dfrac{1}{\Gamma(\alpha+1)}(1-\cos(\pi x))(1-\cos(\pi y)). \end{cases} \quad (53)$$

Substituting Equation (40) into Equation (39) and applying Theorem 1, Definition 6, and properties of CFRDT listed in Table 1, we obtain the following successive iterated values for $k\,(k = 0, 1, 2, \ldots)$.

For $k = 0$, using the values of $U_0(x,y)$ and $U_1(x,y)$ from (53) into (52), we get

$$\begin{aligned} U_2(x,y) &= \frac{\Gamma(1)}{\Gamma(2\alpha+1)}\left[-\frac{\Gamma[\alpha+1]}{\Gamma[1]}U_1(x,y) + \frac{\partial^2}{\partial x^2}U_0(x,y) + \frac{\partial^2}{\partial y^2}U_0(x,y) - 2F_0(x,y) + H_0(x,y)\right] \\ &= \frac{1}{\Gamma(2\alpha+1)}\left[\begin{array}{c} -\dfrac{\Gamma(\alpha+1)}{\Gamma(1)}\dfrac{-1}{\Gamma(\alpha+1)}(1-\cos(\pi x))(1-\cos(\pi y)) + \dfrac{\partial^2}{\partial x^2}(1-\cos(\pi x))(1-\cos(\pi y)) \\ +\dfrac{\partial^2}{\partial y^2}(1-\cos(\pi x))(1-\cos(\pi y)) - 2F_0(x,y) + H_0(x,y) \end{array}\right]. \end{aligned} \quad (54)$$

According to Theorem (1), $F_0(x,y) = \sin U_0 = \sin((1-\cos(\pi x))(1-\cos(\pi y)))$.

Using Definition (5), we get

$$\begin{aligned} H_0(x,y) &= \frac{1}{\Gamma(1)}\left[{}_0^C D_t^0\left[\begin{array}{c} [2\sin(E_\alpha(-t^\alpha)((1-\cos(\pi x))(1-\cos(\pi y))))] \\ -\pi^2 E_\alpha(-t^\alpha)[\cos(\pi x) + \cos(\pi y) - 2\cos(\pi x)\cos(\pi y)] \end{array}\right]\right]_{t=0} \\ &= [2\sin(((1-\cos(\pi x))(1-\cos(\pi y))))] - \pi^2[\cos(\pi x) + \cos(\pi y) - 2\cos(\pi x)\cos(\pi y)]. \end{aligned} \quad (55)$$

Consequently, we obtain

$$U_2(x,y) = \frac{\Gamma(1)}{\Gamma(2\alpha+1)} \begin{bmatrix} (1-\cos(\pi x))(1-\cos(\pi y)) + \pi^2[\cos(\pi x) + \cos(\pi y) - 2\cos(\pi x)\text{co}(\pi y)] \\ -2\sin((1-\cos(\pi x)(1-\cos(\pi y))) + 2\sin(((1-\cos(\pi x)(1-\cos(\pi y))) \\ -\pi^2[\cos(\pi x) + \cos(\pi y) - 2\cos(\pi x)\cos(\pi y)] \end{bmatrix} = \frac{(1-\cos(\pi x))(1-\cos(\pi y))}{\Gamma(2\alpha+1)}, \tag{56}$$

for $k = 1$, using the values of $U_1(x,y)$ and $U_2(x,y)$ in (52), we get

$$U_3(x,y) = \frac{\Gamma[\alpha+1]}{\Gamma(3\alpha+1)} \left[-\frac{\Gamma[2\alpha+1]}{\Gamma[\alpha+1]} U_2(x,y) + \frac{\partial^2}{\partial x^2} U_1(x,y) + \frac{\partial^2}{\partial y^2} U_1(x,y) - 2F_1(x,y) + H_1(x,y) \right] = \frac{\Gamma[\alpha+1]}{\Gamma(3\alpha+1)} \begin{bmatrix} -\frac{\Gamma[2\alpha+1]}{\Gamma[\alpha+1]} \frac{1}{\Gamma(2\alpha+1)} (1-\cos(\pi x))(1-\cos(\pi y)) \\ -\frac{1}{\Gamma(\alpha+1)} \pi^2 [\cos(\pi x) + \cos(\pi y) - 2\cos(\pi x)\cos(\pi y)] - 2F_1(x,y) + H_1(x,y) \end{bmatrix}. \tag{57}$$

According to Theorem (1), we get

$$F_1(x,y) = G_0(x,y)U_1(x,y) = \cos(U_0(x,y))U_1(x,y) = -\frac{1}{\Gamma(\alpha+1)} \cos((1-\cos(\pi x))(1-\cos(\pi y)))(1-\cos(\pi x))(1-\cos(\pi y)). \tag{58}$$

Using Definition (5), we get

$$H_1(x,y) = \frac{1}{\Gamma(\alpha+1)} \left[{}_0^C Dt^{\alpha} \begin{bmatrix} [2\sin(E_\alpha(-t^\alpha)((1-\cos(\pi x))(1-\cos(\pi y)))] \\ -\pi^2 E_\alpha(-t^\alpha)[\cos(\pi x) + \cos(\pi y) - 2\cos(\pi x)\cos(\pi y)] \end{bmatrix} \right]_{t=0} = \frac{1}{\Gamma(\alpha+1)} \begin{bmatrix} \pi^2(\cos(\pi x) + \cos(\pi y) - 2\cos(\pi x)\cos(\pi y)) \\ -2\cos((1-\cos(\pi x))(1-\cos(\pi y)))(1-\cos(\pi x))(1-\cos(\pi y)) \end{bmatrix}. \tag{59}$$

Consequently, we obtain

$$U_3(x,y) = \frac{\Gamma[\alpha+1]}{\Gamma(3\alpha+1)}\begin{bmatrix} -\dfrac{(1-\cos(\pi x))(1-\cos(\pi y))}{\Gamma[\alpha+1]} - \dfrac{\pi^2}{\Gamma(\alpha+1)}[\cos(\pi x)+\cos(\pi y)-2\cos(\pi x)\cos(\pi y)] \\ +\dfrac{2}{\Gamma(\alpha+1)}\cos((1-\cos(\pi x))(1-\cos(\pi y)))(1-\cos(\pi x))(1-\cos(\pi y)) \\ +\dfrac{\pi^2}{\Gamma(\alpha+1)}[\cos(\pi x)+\cos(\pi y)-2\cos(\pi x)\cos(\pi y)] \\ -\dfrac{2}{\Gamma(\alpha+1)}\cos((1-\cos(\pi x))(1-\cos(\pi y)))(1-\cos(\pi x))(1-\cos(\pi y)) \end{bmatrix}$$
$$= -\frac{1}{\Gamma(3\alpha+1)}(1-\cos(\pi x))(1-\cos(\pi y)). \tag{60}$$

Continuing in the same manner for $k \geq 2$, we obtain

$$U_4(x,y) = \frac{1}{\Gamma(4\alpha+1)}(1-\cos(\pi x))(1-\cos(\pi x)), \ldots, U_k(x,y) = \frac{(-1)^k}{\Gamma(k\alpha+1)}(1-\cos(\pi x))(1-\cos(\pi y)). \tag{61}$$

Then, by using inverse CRDT (9), we get

$$\begin{aligned} u(x,y,t) &= \sum_{k=0}^{\infty} U_k(x,y)(t-t_0)^{k\alpha} \\ &= (1-\cos(\pi x))(1-\cos(\pi y))\left[1 - \frac{t^\alpha}{\Gamma(\alpha+1)} + \frac{t^{2\alpha}}{\Gamma(2\alpha+1)} - \frac{t^{3\alpha}}{\Gamma(3\alpha+1)} + \frac{t^{4\alpha}}{\Gamma(4\alpha+1)} - \frac{t^{5\alpha}}{\Gamma(5\alpha+1)} + \cdots\right] \\ &= (1-\cos(\pi x))(1-\cos(\pi y))\left(\sum_{k=0}^{\infty}\frac{(-1)^k (t)^{k\alpha}}{\Gamma(k\alpha+1)}\right). \end{aligned} \tag{62}$$

The Laplace–Padé approximant is used to approximate the truncated series up to n^{th} order of perturbation in this case. That is,

$$\tilde{u}_n(x,y,t) = (1-\cos(\pi x))(1-\cos(\pi y))\left(\sum_{k=0}^{n}\frac{(-1)^k (t)^{k\alpha}}{\Gamma(k\alpha+1)}\right). \tag{63}$$

Then, on both sides of (63), we use the Laplace transform to get

$$L(\tilde{u}_n(x,y,t)) = (1-\cos(\pi x))(1-\cos(\pi y))\left(\sum_{k=0}^{n}\frac{(-1)^k}{s^{\alpha k+1}}\right). \tag{64}$$

For effortlessness, we write $1/t$ instead of $\mathbf{s}$ in Eq., and we get

$$\begin{aligned} L(\tilde{u}_n(x,y,t)) &= (1-\cos(\pi x))(1-\cos(\pi y))\left(\sum_{k=0}^{n}(-1)^k t^{k\alpha+1}\right) \\ &= (1-\cos(\pi x))(1-\cos(\pi y))\left(t - t^{\alpha+1} + t^{2\alpha+1} - t^{3\alpha+1} + t^{4\alpha+1} - t^{5\alpha+1} + t^{6\alpha+1} + \cdots\right). \end{aligned} \tag{65}$$

Now, we convert transformed series (45) into a meromorphic function by forming its Padé approximant of $[K/L]$ with and $K+L=7\,(k=3, L=4)$.

$$\left[\frac{K}{L}\right]\left(t-t^{\alpha+1}+t^{2\alpha+1}-t^{3\alpha+1}+t^{4\alpha+1}-t^{5\alpha+1}+t^{6\alpha+1}\right)=\frac{p_0+p_1t+p_2t^{\alpha+1}+p_3t^{2\alpha+1}}{1+q_1t+q_2t^{\alpha+1}+q_3t^{2\alpha+1}+q_4t^{3\alpha+1}}. \tag{66}$$

We obtain $u_0=0, u_1=1, u_2=-2, u_3=4, u_4=-8, u_5=16, u_6=-32, u_7=64$.

By means of (23) and (22), we get

$$\left\{\begin{array}{ll} p_0=u_0=0, & q_1-q_2+q_3=1,\\ p_1=1, & -q_1+q_2-q_3+q_4=-1,\\ p_2=-1+q_1, & q_1-q_2+q_3-q_4=1,\\ p_3=1-q_1+q_2, & -q_1+q_2-q_3+q_4=-1. \end{array}\right\}\text{ and }. \tag{67}$$

Solving for p and q, we get $p_0=0, p_1=1, p_2=0, p_3=1, q_1=1, q_2=1, q_3=1$, and $q_4=0$.

Then, $[K/L]\,(t-t^{\alpha+1}+t^{2\alpha+1}-t^{3\alpha+1}+t^{4\alpha+1}-t^{5\alpha+1}+t^{6\alpha+1})=t+t^{2\alpha+1}/1+t+t^{\alpha+1}+t^{2\alpha+1}=t/1+t^{\alpha}$.

Therefore, all $[K/L]$ Padé approximants of the equation with $L\geq 1, K\geq 1$ and $K+L\leq n$ give

$$\left[\frac{K}{L}\right]_{\widetilde{u_n}}(x,y,t)=\frac{(1-\cos(\pi x))(1-\cos(\pi y))t}{1+t^{\alpha}}. \tag{68}$$

Now, by changing $1/s$ into $\mathbf{t}$ in the equation, we obtain $[K/L]_{\widetilde{u_n}}$ in terms of $\mathbf{s}$ as follows:

$$\left[\frac{K}{L}\right]_{\widetilde{u_n}}(x,y,t)=\frac{(1-\cos(\pi x))(1-\cos(\pi y))s^{\alpha-1}}{s^{\alpha}+1}. \tag{69}$$

Finally, on both sides of Equation (47), using the inverse Laplace transform, we have the exact solution as follows:

$$\begin{aligned} u(x,y,t)&=(1-\cos(\pi x))(1-\cos(\pi y))L^{-1}\left\{\frac{s^{\alpha-1}}{s^{\alpha}+1}\right\}\\ &=(1-\cos(\pi x))(1-\cos(\pi y))E_{\alpha}(-t^{\alpha}). \end{aligned} \tag{70}$$

Putting $\alpha=1$ in Equation (48), we have

$$\begin{aligned} u(x,y,t)&=(1-\cos(\pi x))(1-\cos(\pi y))L^{-1}\left\{\frac{1}{s+1}\right\}\\ &=e^{-t}(1-\cos(\pi x))(1-\cos(\pi y)). \end{aligned} \tag{71}$$

This finding is in perfect accord with the one obtained in the previous study as shown in [35, 48].

Example 3. Consider the following $(2+1)$–dimensional hyperbolic nonlinear time-fractional telegraph equation with variable coefficients in the area $\Omega=[0,\pi]^2$ as follows:

$$\begin{aligned} &{}_0^C D_t^{2\alpha}u(x,y,t)-u_0^C D_t^{\alpha}u(x,y,t)-u\left(D_x^2u(x,y,t)+D_y^2u(x,y,t)\right)-\left(1+x^2\right)\frac{\partial^2u}{\partial x^2}-\left(1+y^2\right)\frac{\partial^2u}{\partial y^2}\\ &=\left(E_{\alpha}(-t^{\alpha})(\cosh(x)\cosh(y)-\sinh(x+y))-1-x^2-y^2\right)\times E_{\alpha}(-t^{\alpha})\cosh(x)\cosh(y), \end{aligned} \tag{72}$$

with the initial condition

$$\begin{cases} u(x,y,0)=\cosh(x)\cosh(y),\\ {}_0^C D_t^{\alpha}u(x,y,0)=-\dfrac{1}{\Gamma(\alpha+1)}\cosh(x)\cosh(y). \end{cases} \tag{73}$$

Applying the properties of CFRDT and the related rules in Table 1 on both sides of Equation (50), we obtain

$$U_{k+2}(x,y)=\frac{\Gamma(\alpha k+1)}{\Gamma(\alpha k+2\alpha+1)}\begin{bmatrix}\sum_{r=0}^{k}\frac{\Gamma[k\alpha+\alpha+1]}{\Gamma[k\alpha+1]}U_{k+1}(x,y)U_{k-r}(x,y)+\sum_{r=0}^{k}\frac{\partial}{\partial x}U_r(x,y)U_{k-r}(x,y)\\ +\sum_{r=0}^{k}\frac{\partial}{\partial y}U_r(x,y)U_{k-r}(x,y)+\left(1+x^2\right)\frac{\partial^2}{\partial x^2}U_k(x,y)+\left(1+y^2\right)\frac{\partial^2}{\partial y^2}U_k(x,y)\\ +\sum_{r=0}^{k}V_r(x,y)V_{k-r}(x,y)\left[\cosh^2(x)\cosh^2(y)-\sinh(x+y)\cosh(x)\cosh(y)\right]\\ -\frac{(-1)^k}{\Gamma(k\alpha+1)}\left(1+x^2+y^2\right)\cosh(x)\cosh(y)\end{bmatrix}, \tag{74}$$

where $V_k(x,y)$ is the fractional reduced transform of $E_\alpha(-t^\alpha)$.

Applying the CFRDT to initial condition (51) according to Theorem 10, we get

$$\begin{cases}U_0(x,y)=\cosh(x)\cosh(y),\\ U_1(x,y)=-\dfrac{1}{\Gamma(\alpha+1)}\cosh(x)\cosh(y).\end{cases} \tag{75}$$

Now, taking the values of $k(k=0,1,2,\cdots)$ and using Equation (53) into equation (52), we obtain the following successive iterative values.

For $k=0$, using the values of $U_0(x,y)$ and $U_1(x,y)$ from (75) into (74), we get

$$\begin{aligned}U_2(x,y)&=\frac{\Gamma(1)}{\Gamma(2\alpha+1)}\begin{bmatrix}\frac{\Gamma[\alpha+1]}{\Gamma[1]}U_1(x,y)U_0(x,y)+\frac{\partial}{\partial x}U_0(x,y)U_0(x,y)\\ +\frac{\partial}{\partial y}U_0(x,y)U_0(x,y)+\left(1+x^2\right)\frac{\partial^2}{\partial x^2}U_0(x,y)+\left(1+y^2\right)\frac{\partial^2}{\partial y^2}U_0(x,y)\\ +V_0(x,y)V_0(x,y)\left[\cosh^2(x)\cosh^2(y)-\sinh(x+y)\cosh(x)\cosh(y)\right]\\ -\frac{(-1)^0}{\Gamma(1)}\left(1+x^2+y^2\right)\cosh(x)\cosh(y)\end{bmatrix}\\
&=\frac{1}{\Gamma(2\alpha+1)}\begin{bmatrix}-\Gamma[\alpha+1]\frac{1}{\Gamma(\alpha+1)}\cosh(x)\cosh(y)\cosh(x)\cosh(y)+\sinh(x)\cosh(x)\cosh^2(y)\\ +\sinh(y)\cosh(y)\cosh^2(x)+\left(1+x^2\right)\cosh(x)\cosh(y)+\left(1+y^2\right)\cosh(x)\cosh(y)\\ +\cosh^2(x)\cosh^2(y)-\sinh(x+y)\cosh(x)\cosh(y)-\left(1+x^2+y^2\right)\cosh(x)\cosh(y)\end{bmatrix}\\
&=\frac{1}{\Gamma(2\alpha+1)}\begin{bmatrix}-\cosh^2(x)\cosh^2(y)+\sinh(x)\cosh(x)\cosh^2(y)+\sinh(y)\cosh(y)\cosh^2(x)\\ +\cosh^2(x)\cosh^2(y)-\sinh(x)\cosh(x)\cosh^2(y)-\sinh(y)\cosh(y)\cosh^2(x)\\ +\left(1+x^2+y^2\right)\cosh(x)\cosh(y)+\cosh(x)\cosh(y)-\left(1+x^2+y^2\right)\cosh(x)\cosh(y)\end{bmatrix}\\
&=\frac{1}{\Gamma(2\alpha+1)}\cosh(x)\cosh(y).\end{aligned} \tag{76}$$

For $k = 1$, using the values of $U_1(x, y)$ and $U_2(x, y)$ in (74), we get

$$U_3(x,y) = \frac{\Gamma(\alpha+1)}{\Gamma(3\alpha+1)} \left[\begin{array}{c} \sum_{r=0}^{1} \frac{\Gamma[2\alpha+1]}{\Gamma[\alpha+1]} U_2(x,y) U_{1-r}(x,y) + \sum_{r=0}^{1} \frac{\partial}{\partial x} U_r(x,y) U_{1-r}(x,y) \\ + \sum_{r=0}^{1} \frac{\partial}{\partial y} U_r(x,y) U_{1-r}(x,y) + \left(1+x^2\right) \frac{\partial^2}{\partial x^2} U_1(x,y) + \left(1+y^2\right) \frac{\partial^2}{\partial y^2} U_1(x,y) \\ + \sum_{r=0}^{1} V_r(x,y) V_{1-r}(x,y) \left[\cosh^2(x)\cosh^2(y) - \sinh(x+y)\cosh(x)\cosh(y)\right] \\ - \frac{(-1)^1}{\Gamma(\alpha+1)} \left(1+x^2+y^2\right)\cosh(x)\cosh(y) \end{array} \right]$$
$$= \frac{\Gamma(\alpha+1)}{\Gamma(3\alpha+1)} \left[\begin{array}{c} \frac{2}{\Gamma(\alpha+1)} \cosh^2(x)\cosh^2(y) - \frac{2}{\Gamma(\alpha+1)} \sinh(x)\cosh(x)\cosh^2(y) \\ - \frac{2}{\Gamma(\alpha+1)} \cosh(x)\cosh(y)\sinh^2(x) \\ - \frac{1}{\Gamma(\alpha+1)} \cosh(x)\cosh(y) + \frac{1}{\Gamma(\alpha+1)} \left(1+x^2+y^2\right)\cosh(x)\cosh(y) \\ - \frac{2}{\Gamma(\alpha+1)} \cosh^2(x)\cosh^2(y) + \frac{2}{\Gamma(\alpha+1)} \sinh(x)\cosh(x)\cosh^2(y) \\ + \frac{2}{\Gamma(\alpha+1)} \cosh(x)\cosh(y)\sinh^2(x) - \frac{1}{\Gamma(\alpha+1)} \left(1+x^2+y^2\right)\cosh(x)\cosh(y) \end{array} \right]$$
$$= -\frac{1}{\Gamma(3\alpha+1)} \cosh(x)\cosh(y). \tag{77}$$

Continuing in the same manner for $k \geq 2$, we obtain

$$U_4(x,y) = \frac{1}{\Gamma(4\alpha+1)} \cosh(x)\cosh(y), \ldots, U_k(x,y) = \frac{(-1)^k}{\Gamma(k\alpha+1)} \cosh(x)\cosh(y). \tag{78}$$

Then, by (9), we get

$$u(x,y,t) = \sum_{k=0}^{\infty} U_k(x,y)\left(t-t_0\right)^{k\alpha}$$
$$= \cosh(x)\cosh(y)\left[1 - \frac{t^\alpha}{\Gamma(\alpha+1)} + \frac{t^{2\alpha}}{\Gamma(2\alpha+1)} - \frac{t^{3\alpha}}{\Gamma(3\alpha+1)} + \frac{t^{4\alpha}}{\Gamma(4\alpha+1)} - \frac{t^{5\alpha}}{\Gamma(5\alpha+1)} + \cdots\right] \tag{79}$$
$$= \cosh(x)\cosh(y)\left(\sum_{k=0}^{\infty} \frac{(-1)^k (t)^{k\alpha}}{\Gamma(k\alpha+1)}\right).$$

Here, the Laplace–Padé approximant is applied to the truncated series up to n^{th} order of perturbation, that is,

$$\tilde{u}_n(x,y,t) = \cosh(x)\cosh(y)\left(\sum_{k=0}^{n}\frac{(-1)^k (t)^{k\alpha}}{\Gamma(k\alpha+1)}\right). \tag{80}$$

Applying the Laplace transform on both sides of (80) yields

$$L(\tilde{u}_n(x,y,t)) = \cosh(x)\cosh(y)\left(\sum_{k=0}^{n}\frac{(-1)^k}{s^{\alpha k+1}}\right). \tag{81}$$

For simplicity, we write $1/t$ instead of $\mathbf{s}$ i equation (57), we get

$$\begin{aligned} L(\tilde{u}_n(x,y,t)) &= \cosh(x)\cosh(y)\left(\sum_{k=0}^{n}(-1)^k t^{k\alpha+1}\right) \\ &= \cosh(x)\cosh(y)\left(t - t^{\alpha+1} + t^{2\alpha+1} - t^{3\alpha+1} + t^{4\alpha+1} - t^{5\alpha+1} + t^{6\alpha+1} + \cdots\right). \end{aligned} \tag{82}$$

Now, we convert transformed series (58) into a meromorphic function by forming its Padé approximant of $[K/L]$ with $k \geq 1, L \geq 1$, and $K + L = 7\,(k = 3, L = 4)$.

$$\left[\frac{K}{L}\right]\left(t - t^{\alpha+1} + t^{2\alpha+1} - t^{3\alpha+1} + t^{4\alpha+1} - t^{5\alpha+1} + t^{6\alpha+1}\right) = \frac{p_0 + p_1 t + p_2 t^{\alpha+1} + p_3 t^{2\alpha+1}}{1 + q_1 t + q_2 t^{\alpha+1} + q_3 t^{2\alpha+1} + q_4 t^{3\alpha+1}}, \tag{83}$$

We obtain $u_0 = 0, u_1 = 1, u_2 = -2, u_3 = 4, u_4 = -8, u_5 = 16, u_6 = -32, u_7 = 64$.

Using (23) and (22), we get

$$\left\{\begin{array}{lcl} p_0 = u_0 = 0, & & q_1 - q_2 + q_3 = 1, \\ p_1 = 1, & \text{and} & -q_1 + q_2 - q_3 + q_4 = -1, \\ p_2 = -1 + q_1, & & q_1 - q_2 + q_3 - q_4 = 1, \\ p_3 = 1 - q_1 + q_2, & & -q_1 + q_2 - q_3 + q_4 = -1. \end{array}\right\}. \tag{84}$$

Solving for p and q, we get $p_0 = 0, p_1 = 1, p_2 = 0, p_3 = 1, q_1 = 1, q_2 = 1, q_3 = 1$, and $q_4 = 0$.

Then, $[K/L]\,(t - t^{\alpha+1} + t^{2\alpha+1} - t^{3\alpha+1} + t^{4\alpha+1} - t^{5\alpha+1} + t^{6\alpha+1}) = t + t^{2\alpha+1}/1 + t + t^{\alpha+1} + t^{2\alpha+1} = t/1 + t^{\alpha}$.Therefore, all $[K/L]$ Padé approximants of equation (58) with $L \geq 1, K \geq 1$ and $K + L \leq n$ give

$$\left[\frac{K}{L}\right]_{\tilde{u}_n}(x,y,t) = \frac{\cosh(x)\cosh(y)t}{1+t^{\alpha}}. \tag{85}$$

Now, by changing $1/s$ into $\mathbf{t}$ in equation (59, we obtain $[K/L]_{\tilde{u}_n}$ in terms of $\mathbf{s}$ as follows:

$$\left[\frac{K}{L}\right]_{\tilde{u}_n}(x,y,t) = \frac{\cosh(x)\cosh(y)s^{\alpha-1}}{s^{\alpha}+1}. \tag{86}$$

Finally, applying the inverse Laplace transform on both sides of (86), we have the exact solution as follows:

$$\begin{aligned} u(x,y,t) &= \cosh(x)\cosh(y)L^{-1}\left\{\frac{s^{\alpha-1}}{s^{\alpha}+1}\right\} \\ &= \cosh(x)\cosh(y)E_{\alpha}(-t^{\alpha}). \end{aligned} \tag{87}$$

Putting $\alpha = 1$ in the (87), we have

$$\begin{aligned} u(x,y,t) &= \cosh(x)\cosh(y)L^{-1}\left\{\frac{1}{s+1}\right\} \\ &= e^{-t}\cosh(x)\cosh(y). \end{aligned} \tag{88}$$

The obtained result is the same as obtained by Hafez [57].

Example 4. Consider the following $(2+1)$–dimensional hyperbolic time-fractional differential equation in the area $\Omega = [0,1]^2$ as follows:

$$\begin{aligned} {}_0^C D_t^{2\alpha} u(x,y,t) + {}_0^C D_t^{\alpha} u(x,y,t) &= D_x^2 u(x,y,t) + D_y^2 u(x,y,t) + 2\pi^2 u + 2\pi \sin[\pi(x+y)]tE_{\alpha}(-(x+y)t^{\alpha}) \\ &+ \left[(x+y)^2 - (x+y)\right]\sin(\pi x)\sin(\pi y)E_{\alpha}(-(x+y)t^{\alpha}) - 2\sin(\pi x)\sin(\pi y)t^2 E_{\alpha}(-(x+y)t^{\alpha}). \end{aligned} \tag{89}$$

With the initial condition, we obtain

$$\begin{cases} u(x,y,0) = \sin(\pi x)\sin(\pi y), \\ {}_0^C Dt_\alpha^u(x,y,0) = -\dfrac{(x+y)}{\Gamma(\alpha+1)}\sin(\pi x)\sin(\pi y). \end{cases} \quad (90)$$

Applying the CFRDT to initial condition (63) according to Theorem 2, we obtain

$$U_{k+2}(x,y) = \frac{\Gamma(\alpha k+1)}{\Gamma(\alpha k+2\alpha+1)}\begin{bmatrix} -\dfrac{\Gamma[k\alpha+\alpha+1]}{\Gamma[k\alpha+1]}U_{k+1}(x,y) + \dfrac{\partial^2}{\partial x^2}U_k(x,y) + \dfrac{\partial^2}{\partial y^2}U_k(x,y) \\ +2\pi^2 U_k(x,y) + 2\pi\sin[\pi(x+y)]V_k(x,y) \\ +\left[(x+y)^2-(x+y)\right]\sin(\pi x)\sin(\pi y)\dfrac{(-(x+y))^k}{\Gamma(\alpha k+1)} \\ -2\sin(\pi x)\sin(\pi y)W_k(x,y) \end{bmatrix}, \quad (91)$$

where $V_k(x,y)$ and $W_k(x,y)$ are the transformed forms of $tE_\alpha(-(x+y)t^\alpha)$ and $t^2E_\alpha(-(x+y)t^\alpha)$.

Applying the CRDT to initial condition (64), we get

$$\begin{cases} U_0(x,y) = \sin(\pi x)\sin(\pi y), \\ U_1(x,y) = -\dfrac{(x+y)}{\Gamma(\alpha+1)}\sin(\pi x)\sin(\pi y). \end{cases} \quad (92)$$

Substituting equation (66) into equation (65) and applying Definition 9, we obtain the following successive $U_k(x,y)$ values for $k = 0, 1, 2, \ldots$.

$$\begin{aligned} U_2(x,y) &= \frac{\Gamma(1)}{\Gamma(2\alpha+1)}\begin{bmatrix} -\dfrac{\Gamma[\alpha+1]}{\Gamma[1]}U_1(x,y) + \dfrac{\partial^2}{\partial x^2}U_0(x,y) + \dfrac{\partial^2}{\partial y^2}U_0(x,y) + 2\pi^2 U_0(x,y) \\ +2\pi\sin[\pi(x+y)]V_0(x,y) + \left[(x+y)^2-(x+y)\right]\sin(\pi x)\sin(\pi y)\dfrac{(-(x+y))^0}{\Gamma(1)} \\ -2\sin(\pi x)\sin(\pi y)W_0(x,y) \end{bmatrix} \\ &= \frac{\Gamma(1)}{\Gamma(2\alpha+1)}\begin{bmatrix} (x+y)\sin(\pi x)\sin(\pi y) - 2\pi^2\sin(\pi x)\sin(\pi y) + 2\pi^2\sin(\pi x)\sin(\pi y) \\ +(x+y)^2\sin(\pi x)\sin(\pi y)(x+y)\sin(\pi x)\sin(\pi y) \end{bmatrix} \\ &= \frac{(x+y)^2}{\Gamma(2\alpha+1)}\sin(\pi x)\sin(\pi y). \end{aligned}$$

$$
\begin{aligned}
U_3(x,y) &= \frac{\Gamma(\alpha+1)}{\Gamma(3\alpha+1)}\left[\begin{array}{c}
-\frac{\Gamma[2\alpha+1]}{\Gamma[\alpha+1]}U_2(x,y)+\frac{\partial^2}{\partial x^2}U_1(x,y)+\frac{\partial^2}{\partial y^2}U_1(x,y)\\
+2\pi^2U_1(x,y)+2\pi\sin[\pi(x+y)]V_1(x,y)\\
+\left[(x+y)^2-(x+y)\right]\sin(\pi x)\sin(\pi y)\frac{(-(x+y))^1}{\Gamma(\alpha+1)}\\
-2\sin(\pi x)\sin(\pi y)W_1(x,y)
\end{array}\right]\\
&= \frac{\Gamma(\alpha+1)}{\Gamma(3\alpha+1)}\left[\begin{array}{c}
-\frac{\Gamma[2\alpha+1]}{\Gamma[\alpha+1]}\frac{(x+y)^2}{\Gamma(2\alpha+1)}\sin(\pi x)\sin(\pi y)-\frac{\partial^2}{\partial x^2}\frac{(x+y)}{\Gamma(\alpha+1)}\sin(\pi x)\sin(\pi y)\\
-\frac{\partial^2}{\partial y^2}\frac{(x+y)}{\Gamma(\alpha+1)}\sin(\pi x)\sin(\pi y)\\
-2\pi^2\frac{(x+y)}{\Gamma(\alpha+1)}\sin(\pi x)\sin(\pi y)+2\pi\sin[\pi(x+y)]V_1(x,y)\\
+\left[(x+y)^2-(x+y)\right]\sin(\pi x)\sin(\pi y)\frac{(-(x+y))^1}{\Gamma(\alpha+1)}\\
-2\sin(\pi x)\sin(\pi y)W_1(x,y)
\end{array}\right]\\
&= \frac{\Gamma(\alpha+1)}{\Gamma(3\alpha+1)}\left[\begin{array}{c}
-\frac{(x+y)^2}{\Gamma[\alpha+1]}\sin(\pi x)\sin(\pi y)-\frac{2\pi\cos(\pi x)\sin(\pi y)}{\Gamma(\alpha+1)}-\frac{2\pi\sin(\pi x)\cos(\pi y)}{\Gamma(\alpha+1)}\\
+2\pi^2\frac{(x+y)}{\Gamma(\alpha+1)}\sin(\pi x)\sin(\pi y)-2\pi^2\frac{(x+y)}{\Gamma(\alpha+1)}\sin(\pi x)\sin(\pi y)\\
+\frac{2\pi\cos(\pi x)\sin(\pi y)}{\Gamma(\alpha+1)}+\frac{2\pi\sin(\pi x)\cos(\pi y)}{\Gamma(\alpha+1)}\\
-\frac{(x+y)^3}{\Gamma(\alpha+1)}\sin(\pi x)\sin(\pi y)+\frac{(x+y)^2}{\Gamma[\alpha+1]}\sin(\pi x)\sin(\pi y)
\end{array}\right]\\
&= -\frac{(x+y)^3}{\Gamma(3\alpha+1)}\sin(\pi x)\sin(\pi y).
\end{aligned}
\tag{93}
$$

Continuing in the same manner for $k \geq 2$, we obtain

$$U_4(x, y) = \frac{(x+y)^4}{\Gamma(4\alpha+1)} \sin(\pi x)\sin(\pi y), \ldots, U_k(x, y), = (-1)^k \frac{(x+y)^k}{\Gamma(k\alpha+1)} \sin(\pi x)\sin(\pi y). \tag{94}$$

Then, by using inverse CFRDT (9), we get

$$\begin{aligned} u(x, y, t) &= \sum_{k=0}^{\infty} U_k(x, y)(t - t_0)^{k\alpha} \\ &= \sin(\pi x)\sin(\pi y)\left[1 - \frac{(x+y)}{\Gamma(\alpha+1)} t^{\alpha} + \frac{(x+y)^2 t^{2\alpha}}{\Gamma(2\alpha+1)} - \frac{(x+y)^3 t^{3\alpha}}{\Gamma(3\alpha+1)} + \frac{(x+y)^4 t^{4\alpha}}{\Gamma(4\alpha+1)} - \frac{(x+y)^5 t^{5\alpha}}{\Gamma(5\alpha+1)} + \ldots\right] \\ &= \sin(\pi x)\sin(\pi y)\left(\sum_{k=0}^{\infty} \frac{(-1)^k (x+y)^k (t)^{k\alpha}}{\Gamma(k\alpha+1)}\right). \end{aligned} \tag{95}$$

Here, the Laplace–Padé approximant is applied to the truncated series up to n^{th} order of perturbation, that is,

$$\tilde{u}_n(x, y, t) = \sin(\pi x)\sin(\pi y)\left(\sum_{k=0}^{n} \frac{(-1)^k (x+y)^k (t)^{k\alpha}}{\Gamma(k\alpha+1)}\right). \tag{96}$$

Applying the Laplace transform on both sides of (96) yields

$$L(\tilde{u}_n(x, y, t)) = \sin(\pi x)\sin(\pi y)\left(\sum_{k=0}^{n} \frac{(-1)^k (x+y)^k}{s^{\alpha k+1}}\right). \tag{97}$$

For simplicity, we write $1/t$ instead of $\mathbf{s}$ in equation (70), we get

$$\begin{aligned} L(\tilde{u}_n(x, y, t)) &= \sin(\pi x)\sin(\pi y)\left(\sum_{k=0}^{n} (-1)^k (x+y)^k t^{k\alpha+1}\right) \\ &= \sin(\pi x)\sin(\pi y)\left(t - (x+y)t^{\alpha+1} + (x+y)^2 t^{2\alpha+1} - (x+y)^3 t^{3\alpha+1} + \ldots\right). \end{aligned} \tag{98}$$

Now, we convert transformed series (71) into a meromorphic function by forming its Padé approximant of $[K/L]$ with $k \geq 1, L \geq 1$ and $K + L = 7\,(k = 3, L = 4)$.

$$\begin{aligned} &\left[\frac{K}{L}\right]\left(t - (x+y)t^{\alpha+1} + (x+y)^2 t^{2\alpha+1} - (x+y)t^{3\alpha+1} + (x+y)^4 t^{4\alpha+1} - (x+y)^5 t^{5\alpha+1} + (x+y)t^{6\alpha+1}\right) \\ &\quad = \frac{p_0 + p_1 t + p_2 t^{\alpha+1} + p_3 t^{2\alpha+1}}{1 + q_1 t + q_2 t^{\alpha+1} + q_3 t^{2\alpha+1} + q_4 t^{3\alpha+1}}, \end{aligned} \tag{99}$$

We obtain $u_0 = 0, u_1 = 1, u_2 = -2, u_3 = 4, u_4 = -8, u_5 = 16, u_6 = -32, u_7 = 64$.

By using (30) and (31), we get

$$\left\{\begin{array}{l} p_0 = u_0 = 0, \\ p_1 = 1, \\ p_2 = -(x+y) + q_1, \\ p_3 = (x+y)^2 - (x+y)q_1 + q_2, \end{array}\right. \\ \left.\begin{array}{l} (x+y)^2 q_1 - (x+y)q_2 + q_3 = (x+y)^3, \\ -(x+y)^3 q_1 + (x+y)^2 q_2 - (x+y)q_3 + q_4 = -(x+y)^4, \\ (x+y)^4 q_1 - (x+y)^3 q_2 + (x+y)^2 q_3 - (x+y)q_4 = (x+y)^5, \\ -(x+y)^5 q_1 + (x+y)^4 q_2 - (x+y)^3 q_3 + (x+y)^2 q_4 = -(x+y)^6. \end{array}\right\}. \tag{100}$$

Solving for p and q, we get $p_0 = 0, p_1 = 1, p_2 = 0, p_3 = 1, q_1 = (x+y), q_2 = 1, q_3 = (x+y)$ and $q_4 = 0$.

Then, we obtain

$$\begin{aligned} &\left[\frac{K}{L}\right]\left(t - (x+y)t^{\alpha+1} + (x+y)^2 t^{2\alpha+1} - (x+y)^3 t^{3\alpha+1} + (x+y)^4 t^{4\alpha+1} - (x+y)^5 t^{5\alpha+1} + (x+y)^6 t^{6\alpha+1}\right) \\ &= \frac{t + t^{2\alpha+1}}{1 + (x+y)t + t^{\alpha+1} + (x+y)t^{2\alpha+1}} = \frac{t}{1 + (x+y)(t)^{\alpha}}. \end{aligned} \tag{101}$$

Therefore, all $[K/L]$ Padé approximants of equation (84) with $L \geq 1, K \geq 1$ and $K + L \leq n$ give

$$\left[\frac{K}{L}\right]_{\widetilde{u}_n}(x,y,t) = \frac{\sin(\pi x)\sin(\pi y)t}{1 + (x+y)t^{\alpha}}. \tag{102}$$

Now, by changing $1/s$ into $\mathbf{t}$ in equation (72), we obtain $[K/L]_{\widetilde{u}_n}$ in terms of $\mathbf{s}$ as follows:

$$\left[\frac{K}{L}\right]_{\widetilde{u}_n}(x,y,t) = \frac{\sin(\pi x)\sin(\pi y)s^{\alpha-1}}{s^{\alpha} + (x+y)}. \tag{103}$$

To conclude, applying the inverse Laplace transform on both sides of (103), we have the exact solution as follows:

$$\begin{aligned} u(x,y,t) &= \sin(\pi x) in(\pi y) L^{-1}\left\{\frac{s^{\alpha-1}}{s^{\alpha} + (x+y)}\right\} \\ &= \sin(\pi x)\sin(\pi y) E_{\alpha}\left(-(x+y)t^{\alpha}\right). \end{aligned} \tag{104}$$

Putting $\alpha = 1$ in Equation (74), we have

$$u(x,y,t) = \sin(\pi x)\sin(\pi y) L^{-1}\left\{\frac{1}{s + (x+y)}\right\} = e^{-(x+y)t}\sin(\pi x)\sin(\pi y). \tag{105}$$

The obtained result is the same as obtained by Li et al. [48].

6.2. Numerical Simulation to Illustrative Examples. In this subsection, the numerical simulation of the considered problems was depicted using tables and figures. Mathematica software or program has been used to create all 3D figures in this manuscript.

Numerical results corresponding to Example 1 are depicted in Table 2 and Figures 1 and 2.

Numerical results corresponding to Example 2 are depicted in Table 3 and Figures 3 and 4.

Numerical results corresponding to Example 3 are described in Table 4 and Figures 5 and 6.

Numerical results corresponding to Example 4 are depicted in Table 5 and Figures 7 and 8.

7. Discussion

In this article, we showed how to solve the two-dimensional fractional wave equation using the LPCFRDTM. The CFRDTM changed the FPDEs into an easily solvable linear algebraic recursion system for the coefficient functions of the power series solution for each of the fundamental problems

Table 2: Six-term approximate solution by CFRDTM of Example 1 for different values of fractional order α and the absolute error $E = |u_{\text{exact}} - u_{\alpha=1}|$.

t	$\alpha = 0.4$	$\alpha = 0.6$	$\alpha = 0.8$	$\alpha = 1$	Exact	Absolute error $\lvert u_{\text{Exact}} - u_{\alpha=1}\rvert$
0.1	3.929068380	4.495655507	5.323423644	6.049647483	6.049647464	1.83E-08
0.2	4.520577171	3.660230488	4.243334181	4.953034711	4.953032424	2.29E-06
0.3	6.787035081	3.250098689	3.503035478	4.055238123	4.055199967	3.82E-05
0.4	10.98900747	3.182933190	2.966904408	3.320396166	3.320116923	2.79E-04
0.5	17.41731027	3.529929773	2.580183554	2.719583148	2.718281828	1.30E-03
0.6	26.34658866	4.433247113	2.327164227	2.230099888	2.225540928	4.56E-03
0.7	38.03163409	6.083851847	2.220121150	1.835237269	1.822118800	1.31 E-02
0.8	52.70928676	8.712722834	2.296598614	1.524512682	1.491824698	3.27 E-02
0.9	70.60093054	12.58639461	2.619848680	1.294379380	1.221402758	7.30 E-02
1	91.9147090	18.00426917	3.280692948	1.149408727	1	1.49 E-01

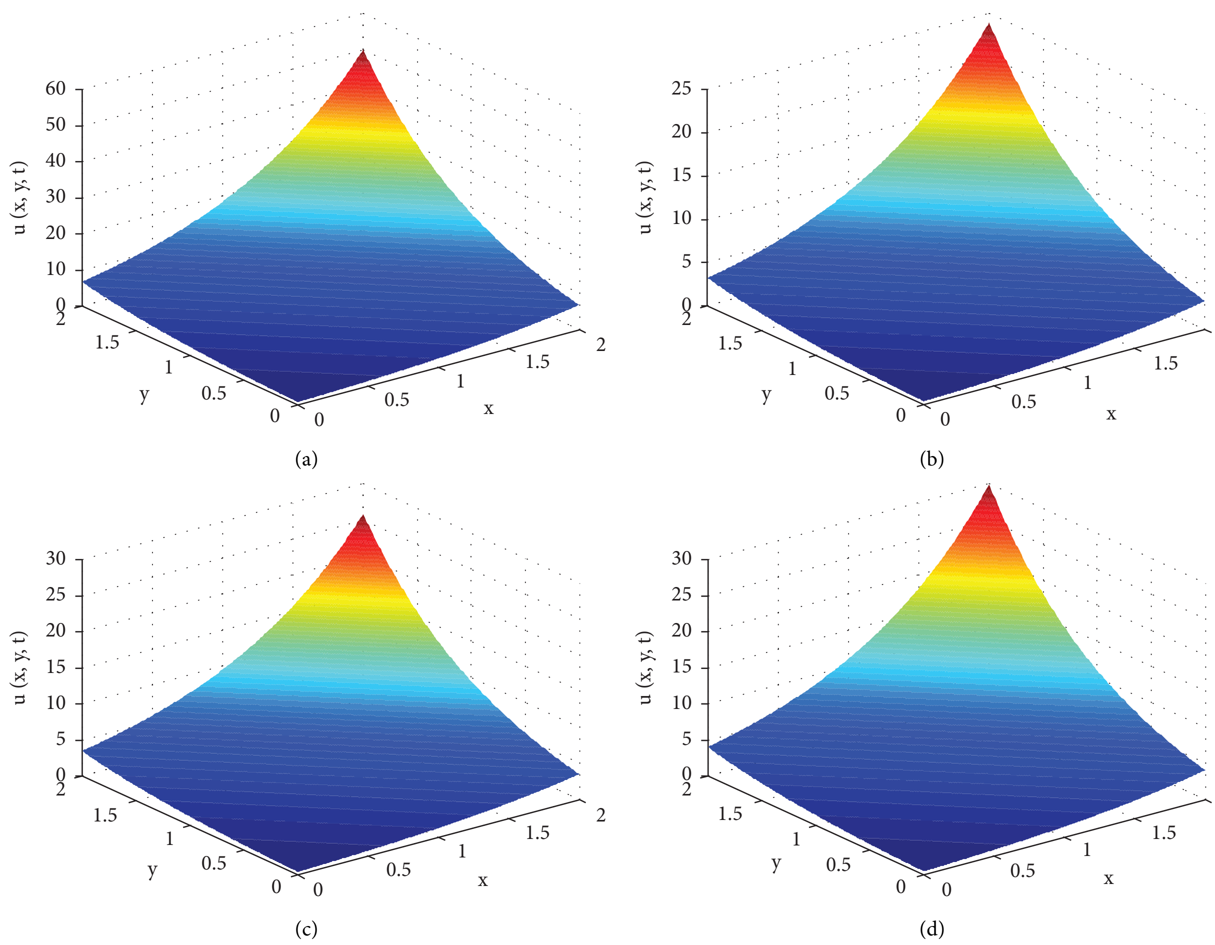

Figure 1: 3D view of the solution behaviour of example 1 at $t = 0.3$ when (a) $\alpha = 0.4$, (b) $\alpha = 0.6$, (c) $\alpha = 0.8$, and (d) $\alpha = 1$.

examined here. The CFRDTM does not require any lengthy computation, which is a major drawback of perturbation methods such as HPM. The main benefit of using this CFRDTM is that it minimizes the computation's size. As previously stated, a Laplace–Padé resummation was applied to the truncated series gained by CFRDTM to increase the domain of convergence of the CFRDTM power series solution, resulting in the precise solution. It is noted that even though the Laplace–Padé resummation technique fails to reach the exact solution of the fractional PDEs under investigation on occasion, it can provide a fair approximation in the larger domain of convergence. Figures 1–8 provide the comparison 3*D* plots of the current solution with the exact solution as well as their related absolute errors, for two test examples at $t = 0.3$ and different values of α. A comparative study between the approximate solution of Examples 1–4 for different values of α and t, at $x = y = 1$, with the exact solutions and their corresponding absolute errors are given in Tables 2–5. As seen in the tables, the proposed approach gives small error near $t = 0$, but the

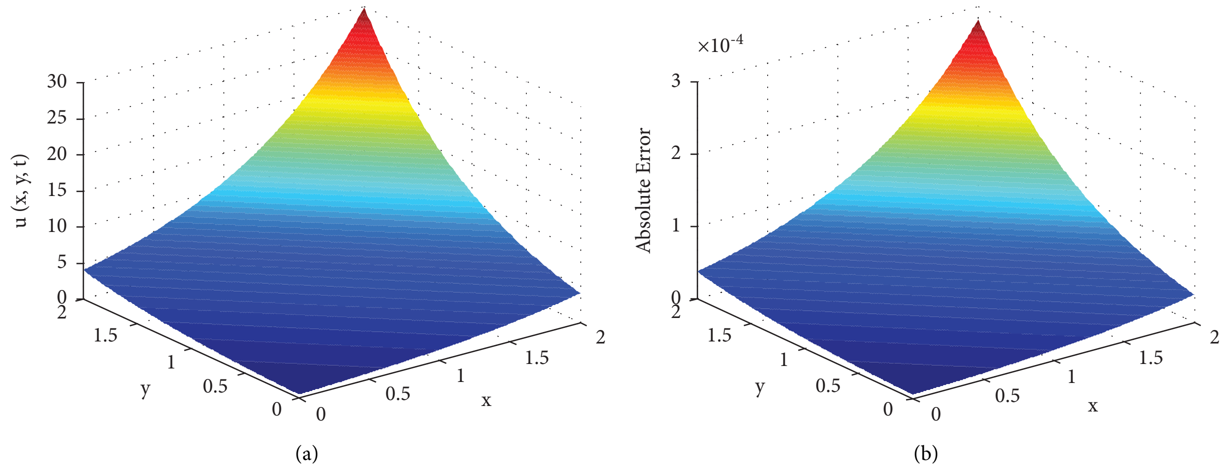

FIGURE 2: 3D view of the solution behaviour of example 1 at $t = 0.3$: (a) exact solution and (b) absolute errors.

TABLE 3: Six-term approximate solutions by CFRDTM of Example 2 for different values of fractional order α and the absolute error $E = |u_{\text{exact}} - u_{\alpha=1}|$.

t	$\alpha = 0.4$	$\alpha = 0.6$	$\alpha = 0.8$	$\alpha = 1$	Exact	Absolute error $\lvert u_{\text{Exact}} - u_{\alpha=1}\rvert$
0.1	2.712457137	3.071502969	3.384587183	3.619349672	3.619349672	7.84E-11
0.2	2.451891233	2.713924889	3.002502404	3.274923022	3.274923012	9.91E-09
0.3	2.300136872	2.469524327	2.703546467	2.963273050	2.963272883	1.67E-07
0.4	2.204166941	2.284239259	2.457455204	2.681281422	2.681280184	1.24E-06
0.5	2.146997592	2.137059874	2.249490775	2.426128472	2.426122639	5.83E-06
0.6	2.121568455	2.017702072	2.070850624	2.195267200	2.195246544	2.07E-05
0.7	2.124684077	1.920678761	1.915742449	1.986401272	1.986341215	6.01E-05
0.8	2.154954324	1.843076134	1.780166233	1.797467022	1.797315856	1.51E-04
0.9	2.211932736	1.783543934	1.661314910	1.626619450	1.626278639	3.41E-04
1	2.295704441	1.741775712	1.557247954	1.472222222	1.471517765	7.04E-03

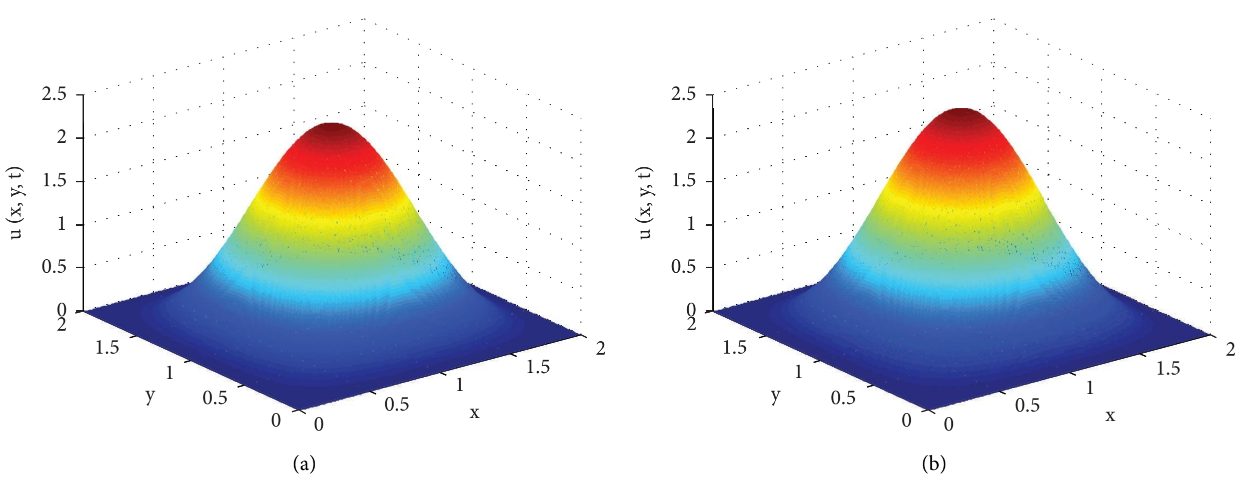

FIGURE 3: Continued.

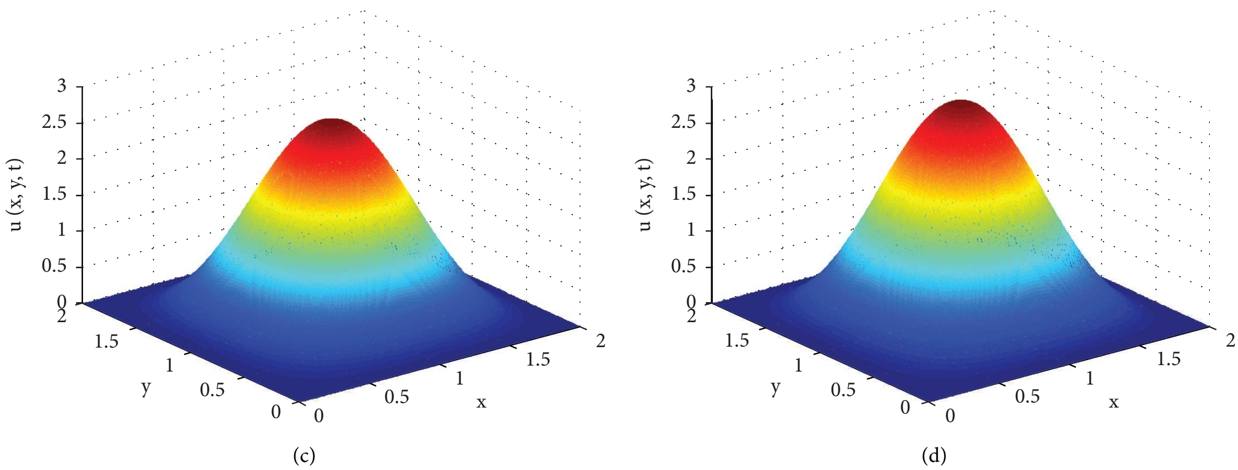

FIGURE 3: 3D view of the solution behaviour of Example 2 at $t = 0.3$ when (a) $\alpha = 0.4$, (b) $\alpha = 0.6$, (c) $\alpha = 0.8$, and (d) $\alpha = 1$.

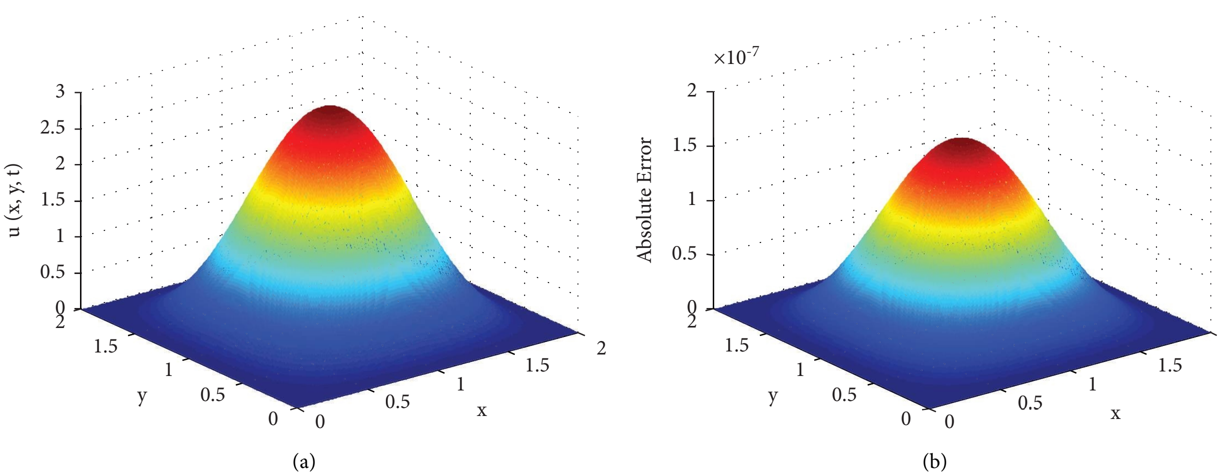

FIGURE 4: 3D view of the solution behaviour of Example 1 at $t = 0.3$: (a) exact solution and (b) absolute errors.

TABLE 4: Six-term approximate solutions by CFRDTM of Example 3 for different values of fractional order α and the absolute error $E = |u_{\text{exact}} - u_{\alpha=1}|$.

t	$\alpha = 0.4$	$\alpha = 0.6$	$\alpha = 0.8$	$\alpha = 1$	Exact	Absolute error $\lvert u_{\text{Exact}} - u_{\alpha=1}\rvert$
0.1	1.614656461	1.828387276	2.014758312	2.154506427	2.154506427	4.67E-11
0.2	1.459548233	1.615530176	1.787313001	1.949478038	1.949478032	5.90E-09
0.3	1.369212737	1.470044764	1.609352167	1.763960769	1.763960669	9.96E-08
0.4	1.312084289	1.359749295	1.462860323	1.596098354	1.596097617	7.37E-07
0.5	1.278052835	1.272137166	1.339064410	1.444212320	1.444208847	3.47E-06
0.6	1.262915519	1.201086514	1.232724490	1.306786500	1.306774204	1.23E-05
0.7	1.264770169	1.143331015	1.140392555	1.182453947	1.182418197	3.58E-05
0.8	1.282789274	1.097136153	1.059687496	1.069986214	1.069896228	9.00E-05
0.9	1.316707068	1.061698154	0.988938338	0.968285017	0.968082141	2.03E-04
1	1.366574224	1.036834599	0.926989937	0.876376290	0.875956945	4.19E-04

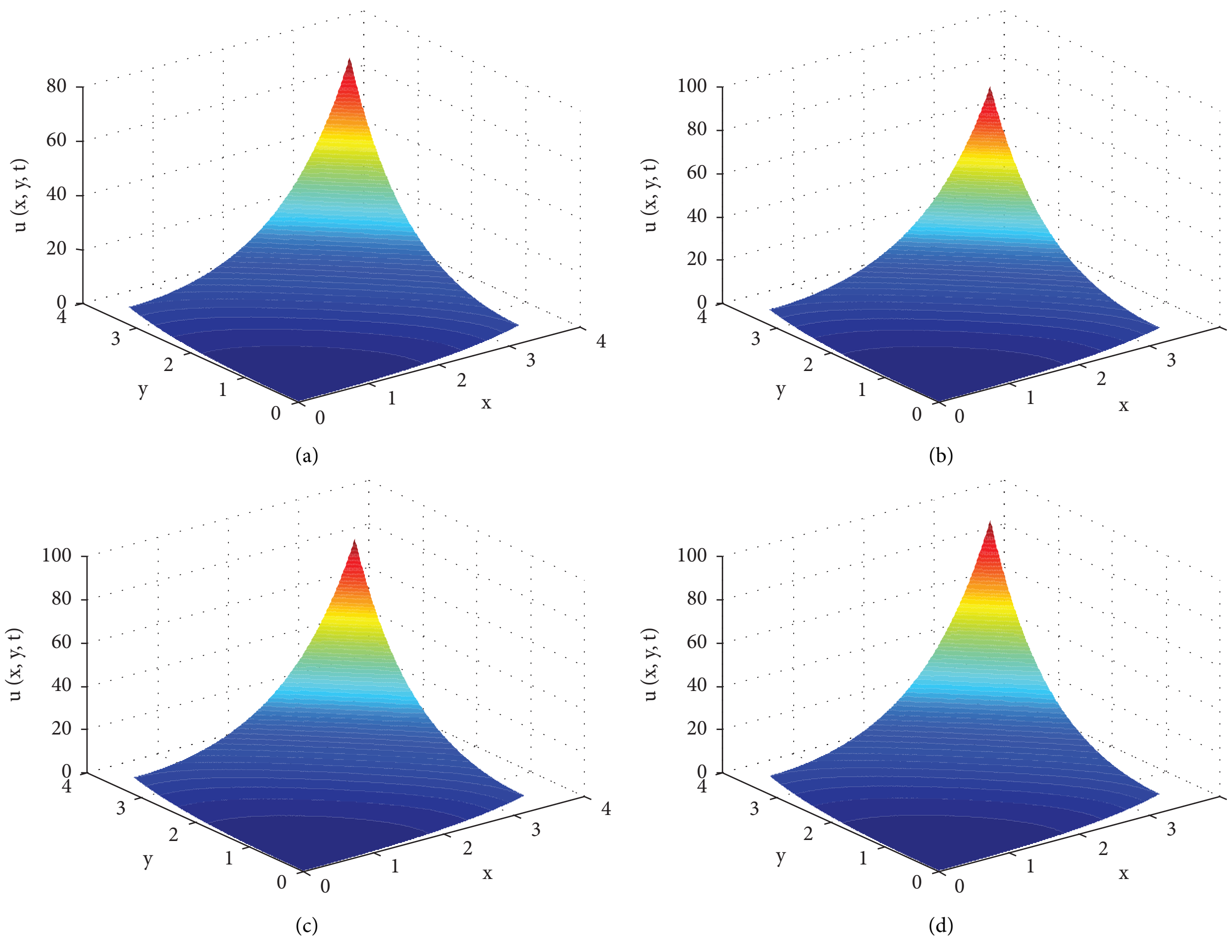

FIGURE 5: 3D view of the solution behaviour of Example 3 at $t = 0.3$ when (a) $\alpha = 0.4$, (b) $\alpha = 0.6$, (c) $\alpha = 0.8$, and (d) $\alpha = 1$.

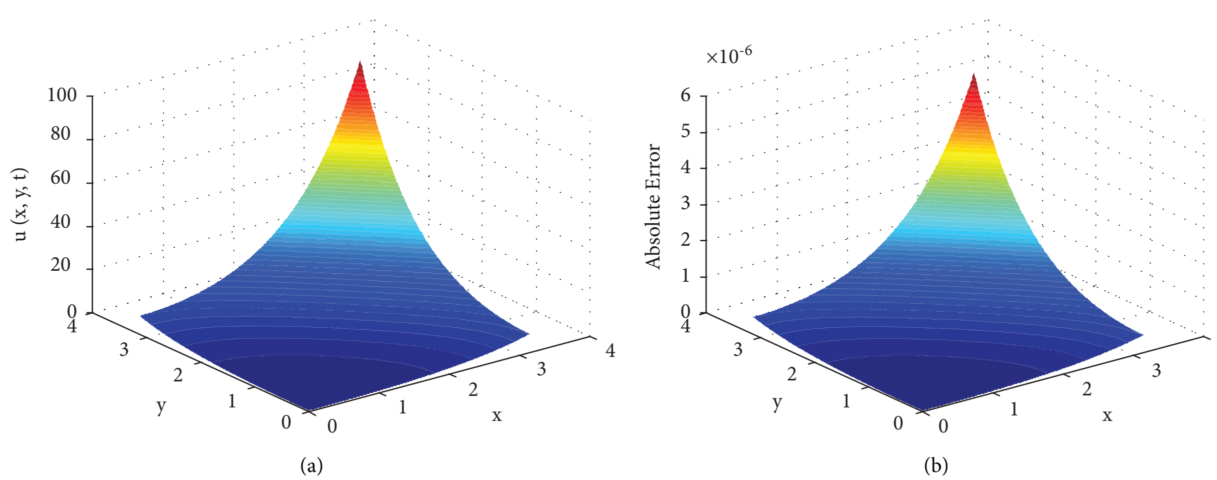

FIGURE 6: 3D view of the solution behaviour of example 3 at $t = 0.3$: (a) exact solution and (b) absolute errors.

Table 5: Six-term approximate solutions by CFRDTM of Example 4 for different values of fractional order α and the absolute error $E = |u_{\text{exact}} - u_{\alpha=1}|$.

t	$\alpha = 0.4$	$\alpha = 0.6$	$\alpha = 0.8$	$\alpha = 1$	Exact	Absolute error $\lvert u_{\text{Exact}} - u_{\alpha=1}\rvert$
0.1	7.97E-33	9.12E-33	1.08E-32	1.23E-32	1.23E-32	3.72E-41
0.2	9.18E-33	7.43E-33	8.61E-33	1.01E-32	1.01E-32	4.64E-39
0.3	1.38E-32	6.60E-33	7.11E-33	8.23E-33	8.23E-33	7.74E-38
0.4	2.23E-32	6.46E-33	6.02E-33	6.74E-33	6.74E-33	5.67E-37
0.5	3.54E-32	7.16E-33	5.24E-33	5.52E-33	5.52E-33	2.64E-36
0.6	5.35E-32	9.00E-33	4.72E-33	4.53E-33	4.54E-33	9.25E-36
0.7	7.72E-32	1.23E-32	4.51E-33	3.72E-33	3.70E-33	2.66E-35
0.8	1.07E-31	1.77E-32	4.66E-33	3.09E-33	3.03E-33	6.63E-35
0.9	1.43E-31	2.55E-32	5.34E-33	2.63E-33	2.48E-33	1.48E-34
1	1.87E-31	3.65E-32	6.66E-33	2.33E-33	2.03E-33	3.03E-34

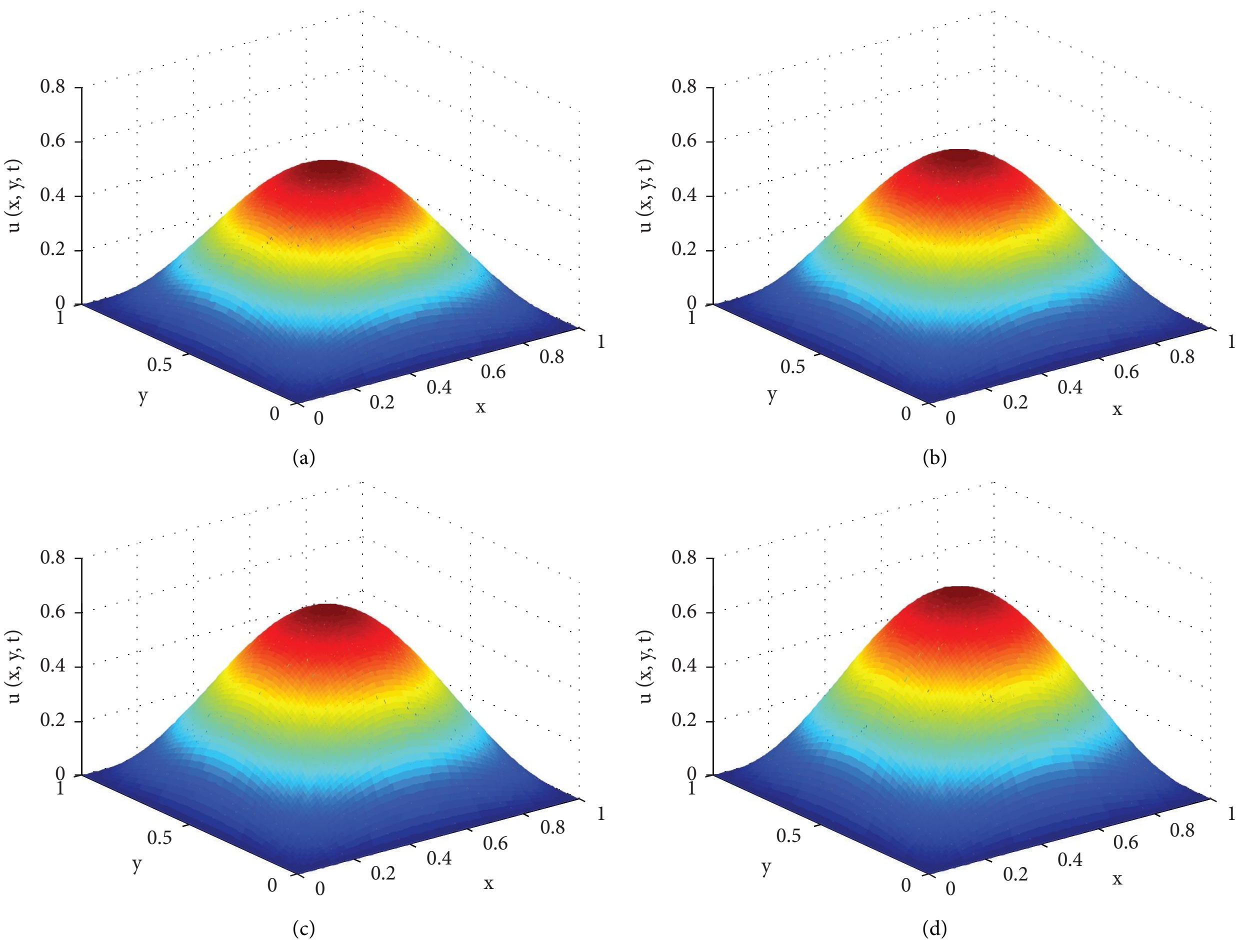

Figure 7: 3D view of the solution behaviour of Example 4 at $t = 0.3$ when (a) $\alpha = 0.4$, (b) $\alpha = 0.6$, (c) $\alpha = 0.8$, and (d) $\alpha = 1$.

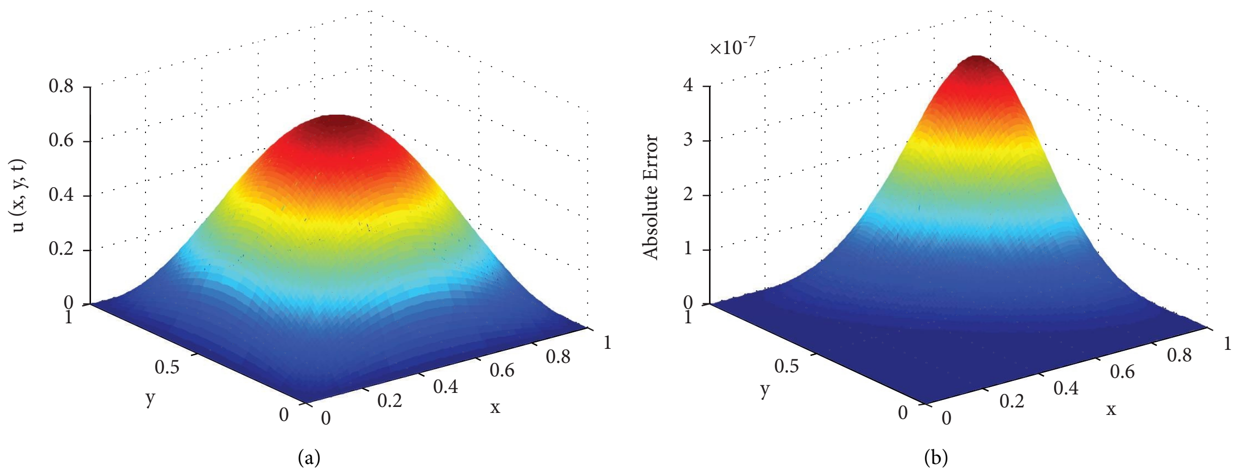

Figure 8: 3D view of the solution behaviour of example 4 at $t = 0.3$: (a) exact solution and (b) absolute errors.

error increases as $|t|$ grows. This means that a superior approximation can be achieved for small values of time t whatever the values of x and y are within the domain of interest.

8. Conclusion

LPCFRDTM, a hybridization of CFRDTM and a resummation method based on Laplace transform and the Padé approximant, was introduced in this paper. First, CFRDTM is used to obtain the solution of two-dimensional NLFPDEs in convergent series form. To extend the domain of convergence of the truncated power series, a post-treatment combining Laplace transforms and the Padé approximant is employed. This approach significantly enhances the convergence rate and yields an exact solution. Furthermore, unlike HPM, CFRDTM is a powerful method because it calculates solutions without taking any perturbation parameters into account. It is evident from the outcomes of instances 1 – 4 that the current procedure produces exact results. As a result, LPCFRDTM is quite valuable, as it allows us to improve accuracy and efficiency and provides a mathematical tool for NLFDEs. Finally, in [54, 58], given the continued use of nonlinear damped differential equations as models in a variety of domains, it is critical to examine this method of solving some intriguing problems in every branch of science and engineering, and we anticipate that this work is a step in that direction.

Data Availability

No data were used to support the study.

Conflicts of Interest

The authors declare that there are no conflicts of interest.

Authors' Contributions

The authors contributed equally to this work.

Acknowledgments

The authors would like to express their gratitude to Mizan Tepi University and Jimma University, the College of Natural Sciences, and the Department of Mathematics for providing the essential resources for this study.

References

[1] M. Alesemi, N. Iqbal, and M. S. Abdo, "Novel analysis of the fractional-order system of non-linear partial differential equations with the exponential-decay kernel," *Mathematics*, vol. 10, no. 4, p. 615, 2022.

[2] C. Xiao, X. Li, Solvability of nonlinear sequential fractional dynamical systems with damping," *Journal of Applied Mathematics and Physics*, vol. 2, 2017.

[3] M. N. Islam, M. M. Miah, M. A. Rahman, and M. A. Akbar, "Adequate closed-form wave solutions to the space time-fractional nonlinear equations in physical sciences," *Partial Differential Equations in Applied Mathematics*, vol. 3, Article ID 100024, 2021.

[4] S. T. R. Rizvi, A. R. Seadawy, K. Ali, M. Younis, and M. A. Ashraf, "Multiple lump and rogue wave for time-fractional resonant nonlinear Schrödinger equation under parabolic law with weak nonlocal nonlinearity," *Optical and Quantum Electronics*, vol. 54, no. 4, pp. 212–114, 2022.

[5] R. M. Jena and S. Chakraverty, "Analytical solution of Bagley–Torvik equations using Sumudu transformation method," *SN Applied Sciences*, vol. 1, no. 3, p. 246, 2019.

[6] A. R. Seadawy, A. Ali, S. Althobaiti, and K. El-Rashidy, "Construction of abundant novel analytical solutions of the space time-fractional nonlinear generalized equal width model via Riemann–Liouville derivative with application of mathematical methods," *Open Physics*, vol. 19, no. 1, pp. 657–668, 2021.

[7] M. Yavuz and N. Özdemir, "Numerical inverse Laplace homotopy technique for fractional heat equations," *Thermal Science*, vol. 22, no. 1, pp. S185–S194, 2018.

[8] A. M. Vargas, "Finite difference method for solving fractional differential equations at irregular meshes," *Mathematics and Computers in Simulation*, vol. 193, pp. 204–216, 2022.

[9] B. Teshome, Y. Obsie, and A. Buseri, "The reduced differential transform method for initial value problem of one dimensional time fractional airy's and airy's type partial differential

equation," *Mathematical Theory and Modeling*, vol. 11, no. 1, p. 18, 2021.

[10] S. E. Fadugba, F. Ali, and A. B. Abubakar, "Caputo fractional reduced differential transform method for SEIR epidemic model with fractional order," *Mathematical Modeling and Computing*, vol. 8, no. 3, pp. 537–548, 2021.

[11] A. T. Deresse, "Analytical solution of one-dimensional nonlinear conformable fractional telegraph equation by reduced differential transform method," *Advances in Mathematical Physics*, vol. 2022, Article ID 7192231, 18 pages, 2022.

[12] M. Richard and W. Zhao, "Padé-sumudu-adomian decomposition method for nonlinear schrödinger equation," *Journal of Applied Mathematics*, vol. 2021, Article ID 6626236, 19 pages, 2021.

[13] A. Khan, A. Khan, T. Khan, and G. Zaman, "Extension of triple Laplace transform for solving fractional differential equations," *Discrete & Continuous Dynamical Systems - S*, vol. 13, no. 3, pp. 755–768, 2020.

[14] H. Eltayeb and I. Bachar, "A note on singular two-dimensional fractional coupled Burgers' equation and triple Laplace Adomian decomposition method," *Boundary Value Problems*, vol. 2020, no. 1, p. 129, 2020.

[15] A. T. Deresse, "Analytical solutions to two-dimensional nonlinear telegraph equations using the conformable triple Laplace transform iterative method," *Advances in Mathematical Physics*, vol. 2022, Article ID 4552179, 17 pages, 2022.

[16] A. T. Deresse, "Double Sumudu transform iterative method for one-dimensional nonlinear coupled sine-gordon equation," *Advances in Mathematical Physics*, vol. 2022, Article ID 6977692, 15 pages, 2022.

[17] P. Karunakar and S. Chakraverty, "Shifted Chebyshev polynomials based solution of partial differential equations," *SN Applied Sciences*, vol. 1, no. 4, p. 285, 2019.

[18] S. O. Edeki, T. Motsepa, C. M. Khalique, and G. O. Akinlabi, "The Greek parameters of a continuous arithmetic Asian option pricing model via Laplace Adomian decomposition method," *Open Physics*, vol. 16, no. 1, pp. 780–785, 2018.

[19] H. Khan, R. Shah, P. Kumam, D. Baleanu, and M. Arif, "Laplace decomposition for solving nonlinear system of fractional order partial differential equations," *Advances in Difference Equations*, vol. 2020, no. 1, p. 375, 2020.

[20] R. M. Jena, S. Chakraverty, and S. K. Jena, "Dynamic response analysis of fractionally damped beams subjected to external loads using homotopy analysis method," *Journal of Applied and Computational Mechanics*, vol. 5, no. 2, pp. 355–366, 2019.

[21] S. K. Elagan, M. Sayed, and M. Higazy, "An analytical study on fractional partial differential equations by Laplace transform operator method," *International Journal of Applied Engineering Research*, vol. 13, no. 1, pp. 545–549, 2018.

[22] Y. Shen and Y. O. El-Dib, "A periodic solution of the fractional sine-Gordon equation arising in architectural engineering," *Journal of Low Frequency Noise, Vibration and Active Control*, vol. 40, no. 2, pp. 683–691, 2021.

[23] L. Akinyemi, M. Senol, and S. N. Huseen, "Modified homotopy methods for generalized fractional perturbed Zakharov–Kuznetsov equation in dusty plasma," *Advances in Difference Equations*, vol. 2021, no. 1, p. 45, 2021.

[24] M. Jneid and A. Chaouk, "The conformable reduced differential transform method for solving Newell-Whitehead-Segel Equation with non-integer order," *Journal of Analysis and Applications*, vol. 18, no. 1, pp. 35–51, 2020.

[25] M. Yavuz and N. Özdemir, "A different approach to the European option pricing model with new fractional operator," *Mathematical Modelling of Natural Phenomena*, vol. 13, no. 1, p. 12, 2018.

[26] M. Eslami and S. A. Taleghani, "Exact solutions of the 3D fractional helmholtz equation by fractional differential transform method," *Journal of Function Spaces*, vol. 2022, Article ID 7374751, 11 pages, 2022.

[27] S. R. Moosavi Noori and N. Taghizadeh, "Modified differential transform method for solving linear and nonlinear pantograph type of differential and Volterra integro-differential equations with proportional delays," *Advances in Difference Equations*, vol. 2020, no. 1, p. 649, 2020.

[28] Ü. Sarp, F. Evirgen, and S. İkikardeş, "Applications of differential transformation method to solve systems of ordinary and partial differential equations," *Journal of Balıkesir University Institute of Science andTechnology*, vol. 20, no. 2, pp. 135–156, 2018.

[29] T. Akturk, Y. Gurefe, and H. Bulut, "New function method to the (n+1)-dimensional nonlinear problems," *An International Journal of Optimization and Control: Theories & Applications*, vol. 7, no. 3, pp. 234–239, 2017.

[30] S. Abuasad, I. Hashim, S. A. Abdul Karim, and A. Karim, "Modified fractional reduced differential transform method for the solution of multiterm time-fractional diffusion equations," *Advances in Mathematical Physics*, vol. 201914 pages, Article ID 5703916, 2019.

[31] S. K. Kebede, "Analytic solutions of time-fractional diffusion equations by fractional reduced differential transform method (FRDTM)," *African Journal of Mathematics and Computer Science Research*, vol. 11, no. 2, pp. 14–34, Article ID E62E34056652, 2018.

[32] V. K. Srivastava, M. K. Awasthi, and S. Kumar, "Analytical approximations of two and three-dimensional time-fractional telegraphic equation by reduced differential transform method," *Egyptian Journal of Basic and Applied Sciences*, vol. 1, no. 1, pp. 60–66, 2014.

[33] P. Jena, S. M. S. Mishra, A. A. Al-Moneef, A. A. Hindi, and K. S. Nisar, "The solution of nonlinear time-fractional differential equations: an approximate analytical approach," *Progress in Fractional Differentiation and Applications*, vol. 8, no. 1, pp. 191–204, 2022.

[34] V. K. Srivastava, M. K. Awasthi, and R. Chaurasia, "Reduced differential transform method to solve two and three-dimensional second-order hyperbolic telegraph equations," *Journal of King Saud university- Engineering sciences*, vol. 29, no. 2, pp. 166–171, 2017.

[35] A. T. Deresse, Y. O. Mussa, and A. K. Gizaw, "Analytical solution of two-dimensional sine-gordon equation," *Advances in Mathematical Physics*, vol. 2021, Article ID 6610021, 15 pages, 2021.

[36] W. G. Belayeh, Y. O. Mussa, and A. K. Gizaw, "Approximate analytic solutions of two-dimensional nonlinear klein–gordon equation by using the reduced differential transform method," *Mathematical Problems in Engineering*, vol. 2020, Article ID 5753974, 12 pages, 2020.

[37] M. Gubes and G. Oturanc, "Approximate solutions of coupled Ramani equation by using RDTM with compared DTM and exact solutions," *New Trends in Mathematical Science*, vol. 4, no. 4, pp. 198–212, 2016.

[38] A. S. J. Al-Saif and A. J. Harfash, "A comparison between the reduced differential transform method and perturbation iteration algorithm for solving two-dimensional unsteady incompressible Navier-Stokes equations," *Journal of Applied Mathematics and Physics*, vol. 6, no. 12, pp. 2518–2543, 2018.

[39] H. Pad, "Thesis: reprsentation approche d'une fonction pour des fractions rationnelles(Representation approximative of a function by a rational function of given order)," *Annales Scientifiques de l'Ecole Normale Superieure*, vol. 9, no. 3, pp. 1–93, 1892.
[40] G. A. Baker, "The existence and convergence of subsequences of Pade approximants," *Journal of Mathematical Analysis and Applications*, vol. 43, no. 2, pp. 498–528, 1973.
[41] N. Özdemir and M. Yavuz, "Numerical solution of fractional black-scholes equation by using the multivariate padé approximation," *Acta Physica Polonica A*, vol. 132, no. 3-II, pp. 1050–1053, 2017.
[42] B. Benhammouda, H. Vazquez-Leal, and A. Sarmiento-Reyes, "Modified reduced differential transform method for partial differential-algebraic equations," *Journal of Applied Mathematics*, vol. 2014, Article ID 279481, 9 pages, 2014.
[43] R. M. Jena and S. Chakraverty, "On the solution of time-fractional coupled system of partial differential equations," *SN Applied Sciences*, vol. 1, no. 12, p. 1655, 2019.
[44] F. Chen and Q. Q. Liu, "Adomian decomposition method combined with padé approximation and Laplace transform for solving a model of HIV infection of $CD4^{+}T$ cells," *Discrete Dynamics in Nature and Society*, vol. 2015, Article ID 584787, 7 pages, 2015.
[45] O. Acan and Y. Keskin, "A new technique of Laplace Pade reduced differential transform method for (1 3) dimensional wave equations," *New Trends in Mathematical Science*, vol. 1, no. 5, pp. 164–171, 2017.
[46] T. R. Ramesh Rao, "Exact solution of gas dynamics equations through reduced differential transform and Sumudu transform linked with pades approximants," *Journal of Physics: Conference Series*, vol. 1000, no. 1, p. 5, Article ID 12107, 2018.
[47] L. Ebiwareme, "Coupling of ¬¬Laplace differential transform method with padé approximant for the numerical solution of initial and boundary value problems," *International Journal of Scientific Research and Management*, vol. 10, no. 3, pp. 373–385, 2022.
[48] D. Li, H. Lai, and B. Shi, "Mesoscopic simulation of the (2 + 1)-dimensional wave equation with nonlinear damping and source terms using the lattice Boltzmann BGK model," *Entropy*, vol. 21, no. 4, p. 390, 2019.
[49] I. Podlubny, "Fractional differential equations," *Mathematics in Science and Engineering*, Vol. 198, Academic Press, San Diego, CA, USA, 1999.
[50] R. Shah, U. Farooq, H. Khan, D. Baleanu, P. Kumam, and M. Arif, "Fractional view analysis of third-order Kortewege–de Vries equations, using a new analytical technique," *Frontiers in Physics*, vol. 7, p. 244, 2020.
[51] U. Farooq, H. Khan, F. Tchier, E. Hincal, D. Baleanu, and H. Bin Jebreen, "New approximate analytical technique for the solution of time-fractional fluid flow models," *Advances in Difference Equations*, vol. 2021, no. 1, pp. 81–20, 2021.
[52] B. R. Sontakke and A. S. Shaikh, "Properties of Caputo operator and its applications to linear fractional differential equations," *International Journal of Engineering Research in Africa*, vol. 5, no. 5, pp. 22–29, 2015.
[53] P. Veeresha, M. Yavuz, and C. Baishya, "A computational approach for shallow water forced Korteweg-De Vries equation on critical flow over a hole with three fractional operators," *An International Journal of Optimization and Control: Theories & Applications*, vol. 11, no. 3, pp. 52–67, 2021.
[54] U. Ayub, S. Mubeen, T. Abdeljawad, G. Rahman, and K. S. Nisar, "The new mittag-leffler function and its applications," *Journal of Mathematics*, vol. 2020, Article ID 2463782, 8 pages, 2020.
[55] Z. Bekiryazici, M. Merdan, and T. Kesemen, "Modification of the random differential transformation method and its applications to compartmental models," *Communications in Statistics - Theory and Methods*, vol. 50, no. 18, pp. 4271–4292, 2021.
[56] I. Andrianov and A. Shatrov, "Padé approximants, their properties, and applications to hydrodynamic problems," *Symmetry*, vol. 13, no. 10, p. 1869, 2021.
[57] R. M. Hafez, "Numerical solution of linear and nonlinear hyperbolic telegraph type equations with variable coefficients using shifted Jacobi collocation method," *Computational and Applied Mathematics*, vol. 37, no. 4, pp. 5253–5273, 2018.
[58] S. A. Bhanotar and M. K. A. Kaabar, "Analytical solutions for the nonlinear partial differential equations using the conformable triple Laplace transform decomposition method," *International Journal of Differential Equations*, vol. 2021, Article ID 6696414, 16 pages, 2021.